NTNU
Norwegian University of
Science and Technology

An Extended CCSD Model Including Triple Excitations for Core-Ionization Energies

Kaja Louise Havig Bredvold

Chemical Engineering and Biotechnology
Submission date: June 2018
Supervisor: Henrik Koch, IKJ
Co-supervisor: Sarai Dery Folkestad, IKJ

Norwegian University of Science and Technology
Department of Chemistry

Abstract. A model for calculation of core-ionization energies is developed within the equations-of-motion coupled cluster framework with application of the CVS approximation. The model deviates from EOM-CCSD by inclusion of triple projection manifold and triple excitation operators, as well as triple excitation amplitudes. However, the triple projection manifold is restricted to only include states involving a specific core excitation, namely an excitation to a super-diffuse orbital. As the super-diffuse orbital does not interact with the molecule orbitals, the model produces core-ionization energies. The truncation level of the cluster operator remains as in EOM-CCSD, but a trivial zero triple cluster operator is added. There are still some minor errors present in the pilot code, but it is expected that the model produces results at an accuracy level close to EOM-CCSDT. The computational cost, however, is reduced to n^7 compared to EOM-CCSDT, which scales as n^8, and could be further reduced to n^6, n denoting the number of basis functions. Since the proposed model is the theoretical equivalent to the experimental procedure XPS, it is named XPS-CCSD. Theoretical spectra may be constructed by core-ionization energies obtained by the XPS-CCSD model, where these are helpful in the interpretation of their experimental counterpart.

Sammendrag. En modell for beregning av kjerneioniseringsenergier er utledet ved hjelp av equations-of-motion coupled cluster teori hvor CVS approksimasjonen er benyttet. Forskjellen mellom denne modellen og eksisterende metoder som EOM-CCSDT og EOM-CCSD er størrelsen på projeksjonsmanifoldet og trunkeringsnivået av cluster-operatoren. Modellen inkluderer de samme elektroninteraksjonene som CCSD, men tar også høyde for trippeleksitasjoner som resulterer i kjerneionisering. En superdiffus orbital er inkuldert i basissettet, slik at kjerneeksitasjon til denne orbitalen resulterer i kjerneionisering. Pilotkoden innholder fremdeles noen små feil, men det er forventet at modellen vil gi resultater som er sammenliknbare med EOM-CCSDT når det kommer til nøyaktighet. Beregningskostnaden er imdilertid redusert til n^7 sammenlignet med EOM-CCSDT som skalerer som n^8, og kan ytterligere reduseres til n^6, hvor n betegner antall basisfunksjoner. Modellen kan brukes til å konstruere teoretiske spekter, hvor et eksperimentelt spekter fra XPS-metoden kan tolkes ved hjelp av det teoretiske spekteret. Derfor har modellen fått navnet XPS-CCSD.

PREFACE. This thesis concludes the master program *Chemical Engineering and Biotechnology* with specialization in *Applied Theoretical Chemistry* at NTNU. It was supervised by Professor Henrik Koch and co-supervised by Sarai D. Folkestad, and written during the spring of 2018. The work was conducted in Trondheim at NTNU, while March was spent at Scuola Normale Superiore di Pisa.

I would like to thank Professor Henrik Koch for his help and advice during this process, as well as the invitation to Pisa. I would also like to thank Sarai D. Folkestad for equation-proof-reading, debugging help and all the knowledge she has shared with me over the past months. I am truly grateful for all the hours she has invested in me, without her guidance the work presented would not have come this far.

Contents

1. Introduction

Quantum mechanical methods yield an accurate description of many-body systems, which includes descriptions of molecular systems and chemical phenomena. A tool for obtaining information about the electronic structure of atoms and molecules is the Schrödinger equation, proposed by Erwin Schrödinger in 1926[1]. Since it is only possible to obtain exact solutions of the Schrödinger equation for the simplest of systems, there have been developed a number of approximate models with different trade-offs between accuracy and computational cost. In this context, *chemical accuracy* is the warranted goal of accuracy in order to achieve predictive quantum chemical models, and involves theoretical values within the range of $\pm$ 1 kcal/mol, or equivalently $\pm$ 0.043 eV, of the corresponding experimental values[2]. However, this goal is in most cases not achieved, such that models tend to only have high accuracy and not fulfil the requirement of being predictive models.

Coupled cluster theory is the foundation of a number of *ab initio* models for electronic structure calculations, where the associated accuracy and computational cost of each model compete. Based on the work on electron correlation by Sinangolu[3] and inspired by the exponential ansatz Coester and Kümmel proposed in connection with nuclear physics[4], the framework of the coupled cluster models was first introduced by Cížek in 1966[5], where equations for the simplest model was derived, and later together with Paldus and Shavitt in 1972[6]. Further development of the framework has since produced models that are widely used for calculation of ground state energies and excitation energies[7–20].

Description of electron correlation in atoms and molecules is considered one of the challenges within the field of quantum chemistry[21], and coupled cluster theory was developed in order to handle this problem. Coupled cluster models retrieve dynamic correlation well, but since the models are based on a single Slater determinant, the description of static correlation is poorer[7;22–24]. Consequently, the coupled cluster models produce accurate results for molecules in the vicinity of their equilibrium geometry, while dissociation energies do not achieve the same level of accuracy. In addition, systems with degenerate or near-degenerate states are also of multireference character, hence coupled cluster models handle such systems poorly as well. There exists an approach

that tries to overcome the multireference issue, namely multireference coupled cluster, abbreviated to MRCC, but this approach is still in development[23;24].

The coupled cluster method involves projection of the coupled cluster Schrödinger equation where the exponential ansatz leads to both connected and disconnected excitation amplitudes. In the resulting equations, the operator used is called the cluster operator and it is parted into terms that induce single excitations, double excitations, triple excitations and so forth, where the non-truncated operator consists of N terms, N denoting the number of electrons, and use of this operator leads to an exact result. The non-truncated operator produces results equal to the results obtained by the full interaction configuration model, FCI, while models with a truncated operator can be associated with the truncated configuration interaction models, CIS, CISD and so forth. In this case, the space used for calculations is not equal to the full space[7;25;26]. However, the computational cost of the coupled cluster model with a non-truncated operator limits it to description of the simplest systems, therefore, the operator is usually truncated, leading to a hierarchy of models, where the computational cost of each model increases with the inclusion of excitation operators in the cluster operator.

The simplest coupled cluster model is called coupled cluster singles, CCS, where the cluster operator is truncated after the first term, corresponding to excitations of a single electron. Including the second term of the cluster operator leads to the CCSD model, where simultaneous excitations of two electrons are considered as well. Continuing in the same manner, the CCSDT model emerges, where the cluster operator consists of the single, double and triple cluster operators. As touched upon earlier, the computational cost of these models increases as the accuracy increases, thus CCSDT will produce more accurate results than CCS and CCSD, which is expected as it includes more electron interactions. The drawback of CCSDT is the computational cost, the model scales as n^8, while CCS scales as n^4 and CCSD as n^6, n denoting the number of basis functions[13;26]. The level of accuracy of CCSDT is often aimed for, but as noted the model is too impractical for application on large systems, creating room for alternative models such as CC3, CCSD(T) and CCSDT-1/2/3[13;16;17].

CC3 is a hybrid model that make use of both coupled cluster theory and perturbation theory, where the coupled cluster wave function is obtained by simplifying the projected coupled cluster amplitude equations by perturbation theory.

The higher order terms, in this case higher than second order, of the perturbation is disregarded in the amplitudes and the determination of the wave function proceeds in the same iterative manner as for CCSDT [13;14;27].

CCSD(T) is not an iterative model such as the rest of the coupled cluster models, it simply adds an correction obtained by perturbation theory to the CCSD energy, thus approximating the CCSDT energy. The correction corresponds to the fourth and fifth order perturbative corrections that contain connected triple amplitudes projected onto the single or double space [14;15;27].

The CCSDT-1/2/3 models include variations of the cluster operator when considering different excitations, for the CCSDT-1 model the exponential cluster operator is approximated by $e^{\hat{T}_1+\hat{T}_2}+\hat{T}_3$, while for CCSDT-2 both $\hat{T}_1$ and $\hat{T}_3$ are neglected when considering the triple excitation amplitude equations and for CCSDT-3 only $\hat{T}_3$ is neglected when considering the triple excitation amplitude equations [16;17].

All of the mentioned models that consider the triple contribution to some extent, CC3, CCSD(T) and CCSDT-1/2/3, scale as n^7, and are often more accurate than CCSD [13–17;27]. CC2 is worth mentioning as an alternative to CCSD, where energies are obtained similarly as for CC3, but in this case the *double* excitation amplitudes are obtained by perturbation theory, leading to a scaling of n^5 [13;27]. The mentioned coupled cluster models are summarised in Table 1.

One approach for describing excitation energies within the coupled cluster framework is to make use of the equations-of-motion theory, EOM-CC, where a parameterization similar to the parameterization in the CI model allows description of excited states [26]. This model was first derived from a time-dependent linear response framework by Monkhorst [28], and later discussed by Emrich [29] and Sekino and Bartlett [30]. A biorthonormal basis and the application of the variational principle results in eigenvalue problems where the solutions provide a good description of the electronic structure. EOM-CC has proved to be one of the most accurate techniques for excited states, and the framework is widely used [31–36].

TABLE 1. Hierarchy of the coupled cluster methods[13–17;26;27]. $\hat{T}$ denotes the cluster operator, while $\hat{T}_i$ denotes the cluster operator containing excitation operators for i electrons.

Model	Cluster operator	Scaling
CCS	$\hat{T} = \hat{T}_1$	n^4
CC2	$\hat{T} = \hat{T}_1$ + perturbative approximations to double excitations	n^5
CCSD	$\hat{T} = \hat{T}_1 + \hat{T}_2$	n^6
CC3	$\hat{T} = \hat{T}_1\hat{T}_2$ + perturbative approximations to triple excitations	n^7
CCSD(T)	$\hat{T} = \hat{T}_1 + \hat{T}_2$ + perturbative approximations added to the CCSD-energy	n^7
CCSDT-1/2/3	$e^{\hat{T}} \approx e^{\hat{T}_1+\hat{T}_2} + \hat{T}_3/e^{\hat{T}} \approx e^{\hat{T}_2}/e^{\hat{T}} \approx e^{\hat{T}_1+\hat{T}_2}$ (the latter two only for triple excitation amplitudes, for single and double $e^{\hat{T}_1+\hat{T}_2+\hat{T}_3}$ is used)	n^7
CCSDT	$\hat{T} = \hat{T}_1 + \hat{T}_2 + \hat{T}_3$	n^8

Another model for description of excited states is the coupled cluster linear response model, abbreviated to CCLR. This approach is based on the time-dependent expectation value of a Hermitian operator where the time-independent coupled cluster linear response function is identified upon expansion[37–39]. In addition to excitation energies, properties such as polarizabilities and oscillator and transition strengths may be obtained by CCLR[40–42].

In order to obtain the eigenvalues of an eigenvalue problem, the Davidson algorithm is often used, this algorithm determines the lowest eigenvalues of large matrices by diagnolising part of the full matrix and projecting onto a suitable subspace[43]. However, other algorithms may be applied as well, for instance the Lanczos algorithm presented by Cornelius Lanczos in 1950[44]. Application of the Davidson algorithm on the EOM-CC eigenvalue problem yields eigenvalues corresponding to the states with the lowest energy, which have emerged by excitation of valence electrons. In order to obtain core excitation energies, the mentioned algorithm is impractical since these final states are of high energy.

Corani and Koch proposed the core valence separation model, abbreviated to CVS, which only takes into account the excitations that involve at least one core orbital in the projection manifold and disregard the other excitations, making determination of the core excitation energies achievable[45].

Introducing a super-diffuse orbital in the basis set, as done by Stanton and Gauss[46], by setting the exponent of the corresponding basis function to nearly zero, makes it possible to determine core-ionization energies. When a core-excited electron excites to the super-diffuse orbital, the final state of the molecule is consisting of one less negative charge, and the molecule is considered ionized. Combining the EOM-CC approach and the CVS model in addition to including a super-diffuse orbital in the basis set introduces an accurate model for core-ionization, which is described in the following chapters.

Table 2 displays core-ionization energies for a selection of coupled cluster models, where experimental values are noted as well. The CCSD(T)(a) model approximates the triple excitation amplitudes differently than what is done in CCSD(T), and corrects the single and double amplitudes as well, which leads to another energy correction added to the CCSD energy as what is the case for CCSD(T), and the model scales as n^7[47].

TABLE 2. Comparison of core-ionization energies for different coupled cluster models. CCSDT numbers are due to Lan Chang at Johns Hopkins, while the rest of the numbers are due to Dr. D. A. Matthews at University of Texas. The basis set used is aug-cc-pCVTZ and energies are given in eV. For the CO molecule, excitations form both core orbitals are considered, denoted by the parenthesis.

	CC2	CCSD	CC3	CCSD(T)(a)	CCSDT	Experimental values[48]
H_2O	537.98	541.48	538.87	539.62	539.61	539.8
CO (O)	540.32	544.27	541.57	542.21	542.26	542.5
CO (C)	297.66	297.62	296.44	296.57	296.43	296.2
NH_3	405.10	407.03	405.17	405.49	405.47	405.6

As observed in Table 2, the core-ionization energies of the different molecules are best described by the CCSDT model, deviation from experimental values is less than 1 eV in every case. The more accurate description provided by CCSDT is expected considering the position of CCSDT in the coupled cluster hierarchy. However, the computational cost of CCSDT is a drawback, and

the perturbative triple excitation models, CC3 and CCSD(T)(a), are both of less computational cost, but both are also less accurate than CCSDT, although CCSD(T)(a) provides energies close to the CCSDT-energies. With this in mind, a model with computational cost less than, or equal to n^7, and that produces as accurate core-ionization energies as CCSDT is warranted.

The theoretical ionization process is equivalent to experimental procedures such as X-ray photoelectron spectroscopy, where the atom or molecule is bombarded by X-rays of the frequency leading to ejection of core-electrons. Construction of such experimental spectra is essential in the determination of molecular and electronic structure, and properties such as charge transfer, geometry, dipole moments, bond angles, bond lengths, and hybridization may be obtained by this approach[45;49]. Such spectra have also been studied theoretically by linear response theory[50;51], density functional theory[52], EOM-CC[53] and other methods[54–56].

The proposed approach contains the single and double projection manifold as in CCSD, but limits the triple projection manifold to only include core-ionizations. Thus, the model includes excitations of a higher level than CCSD, but not all triple excitations are present as in CCSDT. In addition, the cluster operator is truncated after the second term as for CCSD, but the specific triple excitations are present in an additional term added to the truncated operator. However, this term is not equal to the full three-electron part of the cluster operator and is equal to zero as the specific ground state triple excitation amplitudes are equal to zero.

Theoretical preliminaries are covered in Chapter 2, beginning with the second quantization followed by the foundation of coupled cluster theory along with the equations-of-motion technique. Chapter 3 provides a more detailed explanation of the CVS model and the inclusion of a super-diffuse orbital, in addition to a brief overview of the experimental procedures XPS and NEXAFS. While chapter 4 contains the set-up of the derived equations, where the derived equations corresponds to the elements of the Jacobian matrix of the proposed model. The scaling of the proposed model is discussed in Chapter 4. Chapter 5, provides an insight in the implementation of the proposed model, while preliminary results when the model is applied to simple molecules are given in Chapter 6.

2. Theoretical Background

The wave function, Ψ, describes a quantum chemical system and contains in principle all possible information about the system. In order to obtain the wave function, the Schrödinger equation must be solved, here given in its time-independent form,

$$\hat{H}\Psi = E\Psi,$$

where $\hat{H}$ is the Hamiltonian operator and E the energy of the system. An exact solution of this eigenvalue problem is impractical when applied to molecular systems, except for the simplest of systems, and approximations must be made.

2.1. The Second Quantization Representation.

When describing many-body systems, a method that accurately describes changes in the number of particles in the system and particle motion within the system is favourable[57;58]. The second quantization representation is a well-established formalism for this purpose[57;59]. In this representation, the observables and the wave function are both expressed by operators, contrary to the first quantization formulation in quantum chemistry where observables are represented by operators and the wave function has explicit coordinate dependence.

Consider the set of M orthonormal spin orbitals, $\{\phi_P(\mathbf{x}) \mid P = 1, ..., M\}$, where the spin orbitals may be written as a Slater determinant, which is an anti-symmetric product and thus have fulfilled the anti-symmetry of the wave function according to the Pauli principle[60]. A normalized Slater determinant may be written as

$$|\phi_{P_1}\phi_{P_2}\cdots\phi_{P_N}| = \frac{1}{\sqrt{N!}}\begin{vmatrix} \phi_{P_1}(\mathbf{x}_1) & \phi_{P_2}(\mathbf{x}_1) & \cdots & \phi_{P_N}(\mathbf{x}_1) \\ \phi_{P_1}(\mathbf{x}_2) & \phi_{P_2}(\mathbf{x}_2) & \cdots & \phi_{P_N}(\mathbf{x}_2) \\ \vdots & \vdots & \ddots & \vdots \\ \phi_{P_1}(\mathbf{x}_N) & \phi_{P_2}(\mathbf{x}_N) & \cdots & \phi_{P_N}(\mathbf{x}_N) \end{vmatrix},$$

for a system of N electrons. In this notation $\mathbf{x}$ is a coordinate that contains the spatial coordinates, $\mathbf{r}$, and the spin function, σ, of the electron.

Each Slater determinant can be represented by an occupation number vector, $|\mathbf{k}\rangle$, in an abstract linear vector space called the Fock space[61]. The occupation number vectors are basis vectors of the Fock space and contain no spatial structure, and have the form

$$|\mathbf{k}\rangle = |k_1, k_2, ..., k_M\rangle\,, \qquad k_P = \begin{cases} 1 & \text{if } \phi_P \text{ is occupied} \\ 0 & \text{if } \phi_P \text{ is unoccupied.} \end{cases}$$

The number of electrons in the system, N, is thus the sum of the occupation numbers such that $N \leq M$. As a consequence of the orthonormality of the spin orbitals, the inner product of two occupation number vectors produces the Kronecker-delta function[61].

The fundamental building blocks within the second quantization representation are the creation and annihilation operators, and all operators are defined from these[61]. As noted, the state of the system is described by the occupation number vectors, operating the creation operator on such a state for the fermion case yields

$$a_P^\dagger\,|\mathbf{k}\rangle = \delta_{k_P 0}\Gamma_P^{\mathbf{k}}\,|k_1, ..., 1_P, ..., k_M\rangle\,, \tag{1}$$

where $\Gamma_P^{\mathbf{k}} = \prod_{Q=1}^{P-1}(-1)^{k_Q}$ denotes a phase factor. The creation operator, $a_P^\dagger$, creates an electron in spin orbital P by changing the occupation number on site P from 0 to 1. Likewise, the effect of the annihilation operator is

$$a_P\,|\mathbf{k}\rangle = \delta_{k_P 1}\Gamma_P^{\mathbf{k}}\,|k_1, ..., 0_P, ..., k_M\rangle\,. \tag{2}$$

As observed in the above expression, the annihilation operator reduces k_P from 1 to 0 if spin orbital P is occupied. If the mentioned orbital is not occupied the annihilation operator produces zero, since there is no electron to annihilate. The anti-commutation relations of these operators follow from the above relations[57–59;61–63],

$$\begin{aligned} [a_P^\dagger, a_Q^\dagger]_+ &= 0, \\ [a_P, a_Q]_+ &= 0, \\ [a_P^\dagger, a_Q]_+ &= \delta_{PQ}. \end{aligned} \tag{3}$$

As observed in Equations (1) and (2), the creation and annihilation operators alter the number of electrons in the state they operate on. However, when a string of an *equal* number of the creation and annihilation operators operate on a state the procedure is number preserving. The resulting operators are called excitation operators, where the singlet excitation operator, E_{pq}, and the double excitation operator, e_{pqrs}, have the form

$$E_{pq} = a^\dagger_{p\alpha} a_{q\alpha} + a^\dagger_{p\beta} a_{q\beta}, \tag{4}$$

$$e_{pqrs} = E_{pq}E_{rs} - \delta_{qr}E_{ps} = \sum_{\sigma\tau} a^\dagger_{p\sigma} a^\dagger_{r\tau} a_{s\tau} a_{q\sigma}, \tag{5}$$

which are linear combinations of strings of creation and annihilation operators. The permutation symmetry $e_{pqrs} = e_{rspq}$ follows from the definition. Note that the upper case letters in a subscript denote spin orbitals, a combination of spatial and spin part, while lower case letters denote the spatial part such that $\phi_P(\mathbf{x}) = \phi_{p\sigma}(\mathbf{r}, m_s) = \phi_p(\mathbf{r})\sigma(m_s)$, and σ and τ denote general spin functions. In other words, the spin orbital in non-relativistic theory exists in the spin-orbital space, which is spanned by the direct product of a basis for the orbital space and a basis for the spin space. $\phi_p(\mathbf{r})$ is the spatial part of the spin orbital with spatial coordinate $\mathbf{r}$ and $\sigma(m_s)$ is the spin part of the spin orbital with spin coordinate m_s, where m_s is either equal to $\frac{1}{2}$ or $-\frac{1}{2}$ for the fermion case, corresponding to α or β-spin, respectively. Thus, the anti-commutation relation, see Equation (3), may be written as

$$[a^\dagger_{p\sigma}, a_{q\tau}]_+ = \delta_{p\sigma,q\tau} = \delta_{pq}\delta_{\sigma\tau},$$

where creation operator $a^\dagger_{p\sigma}$ is associated with the spin orbital $\phi_{p\sigma}$.

Based on the definitions of the creation and annihilation operators, see Equations (1) and (2) respectively, the electronic Hamiltonian in the second formalism may be expressed as

$$\hat{H} = \sum_{pq} h_{pq}E_{pq} + \frac{1}{2}\sum_{pqrs} g_{pqrs}e_{pqrs} + h_{\text{nuc}}.$$

The operator is valid for the Born-Oppenheimer approximation, such that $\Psi = \psi_{\text{nuc}}\psi_{\text{el}}$ where ψ_{nuc} designates the nuclear wave function and ψ_{el} designates the electronic part of the wave function Ψ. The Hamiltonian in the above expression is also considered non-relativistic, spin-free and in the absence of

external fields[61]. Expressions of the one-integral and two-integral in the expression of the Hamiltonian may be written as

$$h_{pq} = \int \phi_p^*(\mathbf{r}) \left(-\frac{1}{2}\nabla^2 - \sum_I \frac{Z_I}{r_I} \right) \phi_q(\mathbf{r}) \, \mathrm{d}\mathbf{r}, \tag{6}$$

$$g_{pqrs} = \int\int \frac{\phi_p^*(\mathbf{r}_1)\phi_r^*(\mathbf{r}_2)\phi_q(\mathbf{r}_1)\phi_s(\mathbf{r}_2)}{r_{12}} \, \mathrm{d}\mathbf{r}_1 \mathrm{d}\mathbf{r}_2. \tag{7}$$

The expression of the nuclear-repulsion energy, h_{nuc}, in the second formalism is equal to that of the first and is given as

$$h_{\mathrm{nuc}} = \frac{1}{2} \sum_{I \neq J} \frac{Z_I Z_J}{R_{IJ}}, \tag{8}$$

where Z_I denotes the nuclear charge of nucleus I, r_I the distance between an electron and the nucleus, r_{12} the distance between electron 1 and electron 2 and R_{IJ} the distance between nucleus I and nucleus J. Note that the symmetry of the one- and two-electron parameters, see Equation (6) and (7) respectively, is

$$h_{pq} = h_{qp},$$
$$g_{pqrs} = g_{qprs} = g_{pqsr} = g_{qpsr}.$$

for real spin orbitals.

2.2. Coupled Cluster theory. Coupled cluster models are extensively used and provide a relatively accurate approach for description of electronic structure, depending on the level of electron interactions included in the utilised operator[7–12;23;26]. When compared to experimental results, coupled cluster models produce highly accurate results, however, the computational cost is also high. Therefore, these models are only practical for application on small to medium sized molecules. Since the theory is based on a single determinant, as mentioned in Chapter 1, it works well around equilibrium geometry for closed shell systems where it retrieves most of the dynamic correlation[7;22]. Generally, coupled cluster models are size-extensive, due to the exponential cluster operator that guarantees correct scaling with the number of electrons, and few problems concerning optimization occurs[7;26].

The coupled cluster wave function, $|\mathrm{CC}\rangle$, is retrieved by the exponential ansatz,

$$|\mathrm{CC}\rangle = e^{\hat{T}} |\mathrm{HF}\rangle,$$

where the Hartree-Fock state is used as a reference state, which is often the case since coupled cluster models describe correlation, thus coupled cluster models are regarded as post Hartree-Fock models[26]. $\hat{T}$ is called a cluster operator and is a linear combination of excitation operators $\hat{\tau}_\mu$, where the expansion coefficients, t_μ, are called excitation amplitudes and are a probability measure of the associated excitation. Gathering all single excitations in one operator noted as $\hat{T}_1$, all double excitations in another operator noted as $\hat{T}_2$, and so forth, the cluster operator may be written as a sum of these operators,

$$\hat{T} = \hat{T}_1 + \hat{T}_2 + \hat{T}_3 + \ldots + \hat{T}_N,$$

where N is the number of electrons in the system, and $\hat{T}_N$ is an N electron cluster operator containing excitation operators that excite N electrons simultaneously. Truncation of the cluster operator consequently leads to an approximate method, and a hierarchy of approximations is established. All possible electron interactions are taken into account when the non-truncated cluster operator is used, yielding a result equal to that of the full configuration interaction model, FCI[7;26;60].

The truncation level of the cluster operator and its associated models are given in Table 1 in Chapter 1, as well as the scaling of the models, which indicates computational cost. As observed, the computational cost increases with the level of excitations included, n denoting the number of basis functions.

Although the truncation level of CCSD involves no higher than double excitations in the cluster operator, higher level excitations are implicitly included through disconnected excitation amplitudes[7]. Due to the exponential cluster operator, terms on the form $\hat{T}_1\hat{T}_2$ and $\hat{T}_1^3$ emerges when considering the CCSD model, where both terms contribute to an excitation level corresponding to triple excitations. Hence, the triple excitation in CCSD is a process generated by two distinct mechanisms. The associated excitation amplitudes are called disconnected excitation amplitudes and are on the form $t_i^a t_{jk}^{bc}$ and $t_i^a t_j^b t_k^c$, respectively. $a, b, c, \ldots$ denote virtual orbitals, while $i, j, k, \ldots$ denote occupied orbitals. In contrast, the connected triple excitation amplitude in CCSDT has the form t_{ijk}^{abc} and corresponds to simultaneously excitation of three electrons within three orbital pairs. With this in mind, the advantage of the coupled

cluster model is clearly visible; namely the disconnected excitation amplitudes, which give rise to contributions to higher level excitations not directly included in the truncated operator.

As the coupled cluster model is a non-linear parametrization, the variational method results in too complicated expressions for the coupled cluster model. However, within the CI model the variational minimization of the energy is equal to the solution of the projected Schrödinger equation, which indicates an alternative way to obtain an equivalent expression for the non-linear coupled cluster method[26].

Projecting the coupled cluster Schrödinger equation onto the reference state $\langle \mathrm{R}|$ and onto a general projection manifold, $\langle \mu| = \langle \mathrm{R}| \hat{\tau}_\mu^\dagger$, yields

$$\langle \mathrm{R}| e^{-\hat{T}} \hat{H} e^{\hat{T}} |\mathrm{R}\rangle = E, \tag{9}$$

$$\langle \mu| e^{-\hat{T}} \hat{H} e^{\hat{T}} |\mathrm{R}\rangle = 0, \tag{10}$$

where multiplication of $e^{\hat{T}}$ was conducted prior to projection due to simplification. The above expressions remain valid when the cluster operator is truncated[26]. As observed, this alternative scheme introduces the operator $e^{-\hat{T}} \hat{H} e^{\hat{T}}$, which is regarded as the similarity transformed Hamiltonian, designated as $\hat{H}^{\mathrm{T}}$. Note that a similarity transformation does not change the eigenvalues, and that two cluster operators commute, $[\hat{T}_{n_i}, \hat{T}_{n_j}] = 0$ for $n_i, n_j = 1, \ldots, N$. Since the variational principle is not applied in the coupled cluster method, the calculated energy is not an upper bound for the ground state energy.

Upon projection of the coupled cluster Schrödinger equation onto the reference state followed by expansion of the exponential cluster operator, it is established that only the single and double excitation amplitudes contribute to the coupled cluster energy, regardless of the truncation level of the cluster operator. Both the Brillouin theorem and the effect of the Hamiltonian as a two-particle operator enable this result[26]. Nonetheless, the higher level excitation amplitudes contribute indirectly to the energy since all amplitudes are coupled by the projected equations, see Equation (10). For instance, when considering the same system for CCSD and CCSDT, the single and double excitation amplitudes in CCSD may not be equal to the single and double excitation amplitudes in CCSDT, thus the energy may differ as well.

The similarity transformed Hamiltonian is not Hermitian due to that the cluster operator is not anti-Hermitian. Nevertheless, another property of the Hamiltonian is exploited to achieve practical expressions; due to the rank of the operator, a BCH-expansion, see Equation (B.1) in Appendix B, truncates after the fifth term[28]. The truncation level is in accordance with the criterion for surviving commutators given in Appendix D, see Expression (D.1). As a consequence, the non-truncated cluster operator in the projected coupled cluster Schrödinger equation, Equation (10), yields at most quadratic expressions in the excitation amplitudes[26].

Working within the closed-shell CCSD framework, both $\hat{T}_1$ and $\hat{T}_2$ are of singlet symmetry, leading to a spin-adapted method. Compared to the level of excitations included, the CCSD model is a simple method with accurate results, since it is only the single and double excitation amplitudes that contribute directly to the energy, as mentioned earlier. Considering the Brillouin theorem the double excitation amplitudes are the most influential contributors to the total energy, but both the single and double excitation amplitudes are central in obtaining molecular properties, such as the dipole moment[26]. The closed-shell coupled cluster singles and doubles wave function has the form

$$|\mathrm{CCSD}\rangle = e^{\hat{T}_1+\hat{T}_2}\,|\mathrm{R}\rangle,$$

where the one- and two-electron terms of the cluster operator are given in terms of singlet excitation operators, defined in Equation (4),

$$\hat{T}_1 = \sum_{ai} t_i^a E_{ai}, \tag{11}$$

$$\hat{T}_2 = \frac{1}{2}\sum_{aibj} t_{ij}^{ab} E_{ai}E_{bj}. \tag{12}$$

Note that the double excitation amplitudes have the symmetry $t_{ij}^{ab} = t_{ji}^{ba}$. In the CCSD model the similarity transformed Hamiltonian may be written as

$$\hat{H}^{\mathrm{T}} = e^{-\hat{T}_2}\tilde{H}e^{\hat{T}_2} \tag{13}$$

where $\tilde{H}$ is called the $\hat{T}_1$-transformed Hamiltonian. This transformation preserves the particle rank of the Hamiltonian, but there is a loss of symmetry of the one- and two-electron integrals,

$$\tilde{h}_{pq} \neq \tilde{h}_{qp},$$
$$\tilde{g}_{pqrs} = \tilde{g}_{rspq} \neq \tilde{g}_{qprs} \neq \tilde{g}_{pqsr} \neq \tilde{g}_{qpsr}.$$

The above relations hold for both complex and real orbitals. $e^{-\hat{T}_2}\tilde{H}e^{\hat{T}_2}$ can be expanded by the BCH-expansion, and in this case the non-zero nested commutators of the singlet excitation operators and the electronic Hamiltonian applied to the Hartree-Fock state are useful expressions, see Appendix C. The $\hat{T}_1$-transformed Hamiltonian is expressed as

$$\tilde{H} = \sum_{pq} \tilde{h}_{pq} E_{pq} + \frac{1}{2} \sum_{pqrs} \tilde{g}_{pqrs} e_{pqrs} + h_{\text{nuc}},$$

where the one- and two-electron integrals are also $\hat{T}_1$-transformed, the transformation of the excitation operators are encapsulated by the integrals [26]. The $\hat{T}_1$-transformed creation operator is a linear transformed standard creation operator where the two are equal for the unoccupied case. Likewise, the $\hat{T}_1$-transformed annihilation operator is a linear transformed standard annihilation operator where the two are equal for the occupied case.

2.3. Equation-of-Motion Coupled Cluster theory. The coupled cluster framework was originally developed in order to describe the ground state, whereas the goal of the equation-of-motion coupled cluster model, EOM-CC, is to describe the electronic structure of the excited states as accurate as the structure of the ground state. Consequently, the model is widely used to obtain excitation energies [8;31–33;36], but it may also be applied for ionization potentials [8;46;64–68] and electron attachments [8;68–70]. The model provides an accurate spin-adapted final state wave function when applied to a closed-shell reference state, and as long as the cluster operator is not truncated the EOM-CC method is an exact procedure [31].

The basis of the EOM-CC model is a CI-type linear parameterization of the excited states on the form

$$|\mathbf{c}) = \sum_{\mu} c_\mu \hat{\tau}_\mu |\text{CC}\rangle = e^{\hat{T}} \sum_{\mu} c_\mu \hat{\tau}_\mu |\text{R}\rangle,$$

where the ground state is also included in the summation. In the EOM-CC model the bra and ket states form a biorthonormal set, where a biorthonormal

set consists of two sets that are orthogonal to each other, but the two sets are not orthogonal among themselves[31]. The biorthonormal set may be written as

$$|\mu) = e^{\hat{T}} |\mu\rangle \,, \tag{14}$$

$$(\mu| = \langle\mu| \, e^{-\hat{T}}, \tag{15}$$

in the EOM-CC basis. The orthonormality of the determinants in the spin-orbital basis leads to biorthnormality[31],

$$\langle\mu|\nu\rangle = (\mu|\nu) = \delta_{\mu\nu}.$$

In the EOM-CC model the energy can be expressed as a pseudo-expectation value, which is minimized in accordance with the variational principle in order to determine the states. Thus, the following eigenvalue equations are produced

$$\mathbf{H}\mathbf{c} = E\mathbf{c}, \tag{16}$$

$$\overline{\mathbf{c}}^{\mathrm{T}}\mathbf{H} = \overline{\mathbf{c}}^{\mathrm{T}}E, \tag{17}$$

where the elements of the non-symmetric real matrix $\mathbf{H}$ is given by $H_{\mu\nu} = (\mu|\hat{H}|\nu)$ and $\mathbf{c}$ and $\overline{\mathbf{c}}$ are column vectors containing the expansion coefficients c_ν and $\overline{c}_\mu$. Since the bra- and ket-coefficients are numerically different, the bra-states are denoted with overbars. It is possible to choose the eigenvectors such that they are orthogonal, $\overline{\mathbf{c}}_i^{\mathrm{T}}\mathbf{c}_j = \delta_{ij}$. Thereby, the calculation of the EOM-CC states is reduced to diagonalising a non-symmetric matrix. The eigenvalues may become complex since the similarity transformed Hamiltonian is not Hermitian. Nevertheless, when the biorthonormal set of expansion coefficients, which carries information about the excitation structure of the electronic states, provides a good representation the eigenvalues will be real[26].

For the optimized coupled cluster ground state, with energy E_0, the Hamiltonian matrix has a special structure,

$$(\mu|\hat{H}|\mathrm{R}) = \begin{cases} E_0 & \mu = 0 \\ 0 & \mu > 0, \end{cases} \tag{18}$$

where the first case is in accordance with definitions given in Equation (14) and (15). While the second case is valid due to orthogonality. An element of the

non-symmetric matrix $\mathbf{H}$ that corresponds to the excited projection manifold may be written as

$$\begin{aligned} H_{\mu\nu} = (\mu|\hat{H}|\nu) &= \langle \mathrm{R}| \hat{\tau}_\mu^\dagger [\hat{H}^\mathrm{T}, \hat{\tau}_\nu] |\mathrm{R}\rangle + \langle \mathrm{R}| \hat{\tau}_\mu^\dagger \hat{\tau}_\nu \hat{H}^\mathrm{T} |\mathrm{R}\rangle \\ &= (\mu|[\hat{H}, \hat{\tau}_\nu]|\mathrm{R}) + \delta_{\mu\nu} E_0. \end{aligned}$$

Thereby the EOM-CC Hamiltonian matrix may be expressed as a block structured matrix,

$$\mathbf{H} = \begin{pmatrix} 0 & \boldsymbol{\eta}^\mathrm{T} \\ 0 & \mathbf{A} \end{pmatrix} + E_0 \mathbf{1},$$

for an optimized coupled cluster state[26]. The elements of the column vector $\boldsymbol{\eta}$ is given as $(\mathrm{R}|\hat{H}|\mu)$. While the elements of the coupled cluster Jacobian matrix $\mathbf{A}$ is given as

$$A_{\mu\nu} = (\mu|[\hat{H}, \hat{\tau}_\nu]|\mathrm{R}). \tag{19}$$

Note that this matrix is also a non-symmetric matrix. The eigenvalue equations, Equations (16) and (17), may be simplified by level-shifting, where the the ground state energy is subtracted, such that $\Delta\mathbf{H} = \mathbf{H} - E_0\mathbf{1}$ and $\Delta E = E - E_0$[26]. As a consequence, the non-zero eigenvalues correspond to the excitation energies while the eigenvectors of $\Delta\mathbf{H}$ are the same as for $\mathbf{H}$. Considering an excited state K, the following eigenvalue equations are obtained

$$\mathbf{A}\mathbf{t}_K = \Delta E_K \mathbf{t}_K, \tag{20}$$

$$\bar{\mathbf{t}}_K^\mathrm{T} \mathbf{A} = \bar{\mathbf{t}}_K^\mathrm{T} \Delta E_K, \tag{21}$$

by multiplying the emerging matrices. $\mathbf{t}_K$ is a column vector containing coefficients for the excited states, thereby, the excitation energies are the eigenvalues of the coupled cluster Jacobian. As noted previously the eigenvalues may become complex since the Jacobian is a non-symmetric matrix. However, whenever a suitable ground state wave function is used this is not a problem. There is one drawback of the above eigenvalue problems, the first column of the shifted Hamiltonian matrix, $\Delta\mathbf{H}$, have to vanish in order for the EOM-CC equations for the excited states to work properly. For CCSD and CCSDT this

criteria is fulfilled since the first column vanish due to the that the amplitude equations, see Equation (10), are satisfied. However, this criterion makes the EOM-CC model limited in use[26].

In closed-shell CCSD the Jacobian matrix, $\mathbf{A}^{\mathrm{CCSD}}$, has the form

$$\mathbf{A}^{\mathrm{CCSD}} = \begin{pmatrix} \langle \mu_1 | \left[\hat{H}^T, \hat{\tau}_{\nu_1}\right] | \mathrm{HF} \rangle & \langle \mu_1 | \left[\hat{H}^T, \hat{\tau}_{\nu_2}\right] | \mathrm{HF} \rangle \\ \langle \mu_2 | \left[\hat{H}^T, \hat{\tau}_{\nu_1}\right] | \mathrm{HF} \rangle & \langle \mu_2 | \left[\hat{H}^T, \hat{\tau}_{\nu_2}\right] | \mathrm{HF} \rangle \end{pmatrix}, \tag{22}$$

as in accordance with Equation (19). In this case, $\hat{\tau}_{\nu_1} = E_{bj}$ and $\hat{\tau}_{\nu_2} = E_{bj}E_{ck}$, as observed in Equation (11) and Equation (12), respectively. The Jacobian matrix for the closed-shell CCSDT model has the form

$$\mathbf{A}^{\mathrm{CCSDT}} = \begin{pmatrix} \langle \mu_1 | \left[\hat{H}^T, \hat{\tau}_{\nu_1}\right] | \mathrm{HF} \rangle & \langle \mu_1 | \left[\hat{H}^T, \hat{\tau}_{\nu_2}\right] | \mathrm{HF} \rangle & \langle \mu_1 | \left[\hat{H}^T, \hat{\tau}_{\nu_3}\right] | \mathrm{HF} \rangle \\ \langle \mu_2 | \left[\hat{H}^T, \hat{\tau}_{\nu_1}\right] | \mathrm{HF} \rangle & \langle \mu_2 | \left[\hat{H}^T, \hat{\tau}_{\nu_2}\right] | \mathrm{HF} \rangle & \langle \mu_2 | \left[\hat{H}^T, \hat{\tau}_{\nu_3}\right] | \mathrm{HF} \rangle \\ \langle \mu_3 | \left[\hat{H}^T, \hat{\tau}_{\nu_1}\right] | \mathrm{HF} \rangle & \langle \mu_3 | \left[\hat{H}^T, \hat{\tau}_{\nu_2}\right] | \mathrm{HF} \rangle & \langle \mu_3 | \left[\hat{H}^T, \hat{\tau}_{\nu_3}\right] | \mathrm{HF} \rangle \end{pmatrix}, \tag{23}$$

as in accordance with Equation (19). In the above matrix the triple excitation operator $\hat{\tau}_{\nu_3}$ equals $E_{bj}E_{ck}E_{dl}$, while $\hat{\tau}_{\nu_1}$ and $\hat{\tau}_{\nu_2}$ are equal to the corresponding terms for the CCSD case.

Note that the Hamiltonian matrix is non-symmetric within EOM-CC theory, subsequently the left and right eigenvectors differ. As a consequence, the EOM-CC model is not size-intensive when considering transition properties such as dipole transition strengths, oscillator strengths and rotational strengths, and CCLR and EOM-CC will thus provide different results[41;42]. When considering the FCI-limit, however, EOM-CC will produce the same result as CCLR. Both EOM-CC and CCLR are size-intensive when considering excitation energies, thus the two models provide the same results in this case.

3. Background on the proposed model and link to experimental procedures

EOM-CC is a model designed for obtaining excitation energies of a molecular system, where the Davidson algorithm is utilised in order to obtain valence excitation energies. The Davidson algorithm is a procedure for obtaining the lowest eigenvalues of a large real-symmetric matrix[43], but a generalized version may be applied to non-symmetric matrices, which might produce complex eigenvalues. Thus this approach can be applied to the Jacobian eigenvalue problem, see Equations (20) and (21), in order to calculate the lowest excitation energies. With this in mind, the Davidson algorithm is not applicable for obtaining excitation energies when considering core excitations, since such excitations are of high energy and the Davidson algorithm applies a bottom-up approach.

In order to retrieve core excitation energies the CVS model has proved an accurate approach[45;71;72]. The foundation of the CVS model is a core-valence separation consisting of projecting out all excitations that do not contain at least one core excitation. Separation of core and valence-electrons was first proposed by Cederbaum, Domcke and Schirmer[73] where the Hamiltonian was split into two terms that treated core and valence electrons separately. The justification of this separation is the large difference in both energy and localization in space between the core and valence electrons.

Stanton and Gauss added a super-diffuse orbital to the set of unoccupied molecular orbitals and recognised that an excitation of an electron to the super-diffuse orbital portrayed an ionization process. Core-ionization energies were obtained by applying the approach for several CCSDT methods[46]. The resulting ionization energies proved to be in agreement with experimental values, thus a simple method for obtaining ionization energies was presented. A final state containing $N-1$ electrons, which corresponds to the diagonal representation of $\hat{H}^{\mathrm{T}}$ in the $N-1$ electron Hilbert space, can be demonstrated to be identical to a restricted N electron excited state treatment when a super-diffuse orbital is included in the basis set[46;64]. Likewise, an electron attachment process can be described by EOM-CC where the final state contains $N+1$ electrons[64]. This method is often called EA-EOM-CC and is among others presented by Nooijen and Bartlett[69].

Adding a super-diffuse orbital to the basis set and applying the CVS technique in addition to restricting the core excitations to only involve excitations to the

mentioned orbital, makes it possible to obtain core-ionization energies within the EOM-CC framework. Restricting the triple excitations to only include the specific core excitation, leads to a Jacobian matrix with more elements than the CCSD Jacobian matrix, but the elements will differ from the elements of the CCSDT Jacobian matrix, which is the case for the proposed model.

3.1. Spectroscopy. The field of spectroscopy is based on the interaction of electromagnetic radiation with matter, where absorption and emission properties of molecules or atoms make it possible to obtain an accurate description of the molecular or atomic structure[49;74]. Transition between two states of a particle may be induced by electromagnetic radiation and this process is described theoretically by quantum mechanics, where the Franck-Condon principle states that the momentum and position of the nuclei will not change significantly due to an electronic transition since such transitions are so fast compared to the motion of the nuclei[74]. As a consequence, the turning point belonging to the vibrational state vertically above the internuclear equilibrium separation of the ground state will give rise to the most intense absorption.

An example of the corresponding Franck-Condon diagram is visualized in Figure 1, where the green arrow represents the vertical transition, the energy of such a transition is called the vertical excitation energy, and these energies are usually considered when estimating excitation energies since the assumption of no geometrical changes simplifies the calculation. The excitations in the proposed model are considered vertical, leading to a vertical ionization energy.

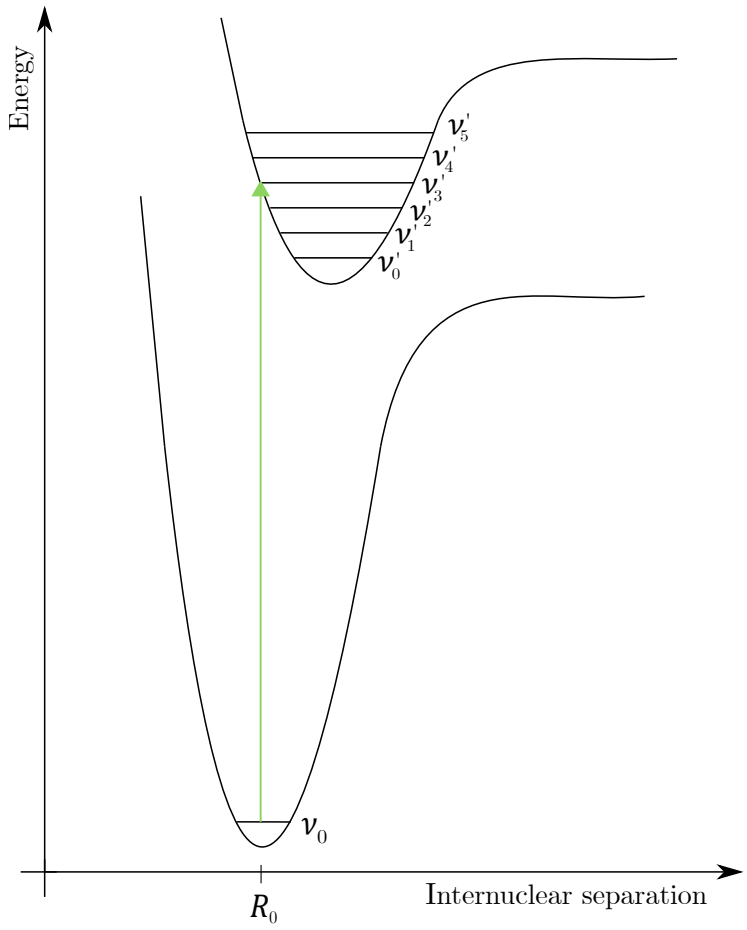

FIGURE 1. An illustration of a vertical excitation, adapted after figures in chapter 5 of *Symmetry and Spectroscopy*[74]. The green arrow visualises the vertical excitation from vibrational state ν_0 to the excited vibrational state ν_3'. Along the vertical axis the energy of the system is noted, while the internuclear separation is noted along the horizontal axis, where R_0 denotes the internuclear equilibrium separation.

There exists a wide range of experimental spectroscopic procedures, based on what kind of system that is studied and what the property in question is. In X-ray photoelectron spectroscopy, abbreviated to XPS, the atom or molecule is bombarded by monochromatic photons of the frequency leading to ejection of core-electrons, where an ejected electron is called a photoelectron[49]. This process is visualised schematically in Figure 2.

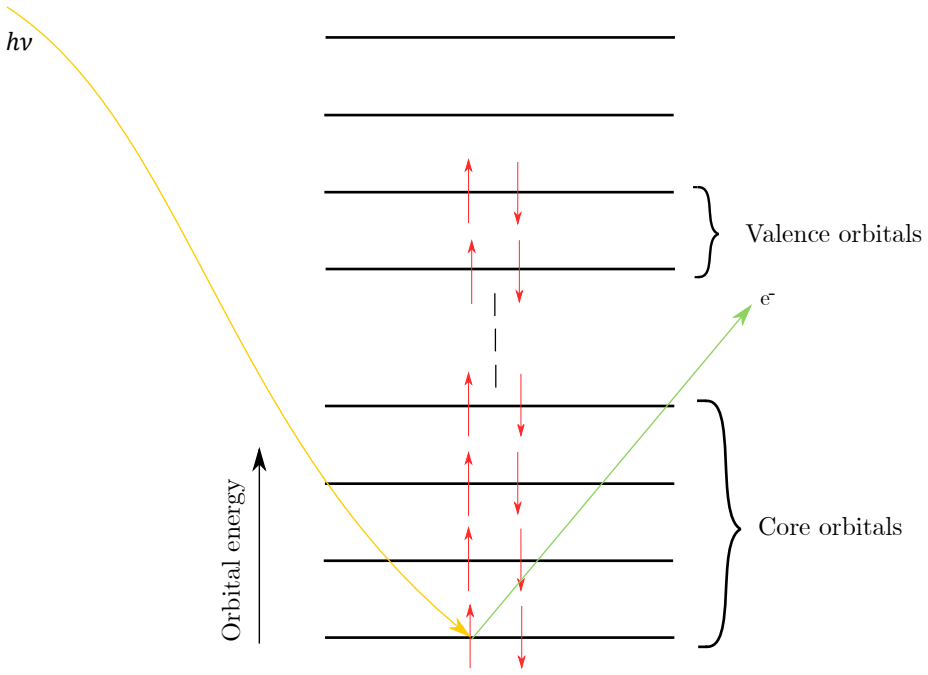

FIGURE 2. The XPS process visualised schematically, adapted after figure 8.1 in chapter 8 of *Modern Spectroscopy*[49]. An electron initially in the core orbital is ejected from the atom or molecule, illustrated by the green arrow, when the system is subject to X-rays of energy $h\nu$ illustrated by the yellow arrow. h denotes the Planck constant and ν the frequency, while e^- denotes an electron.

Separating the photoelectrons in relation to their kinetic energy and measuring the number of electrons per unit time trough a slit, makes it possible to construct a spectrum. Similarly, the NEXAFS, near edge X-ray absorption fine structure, technique studies the electronic structure of molecules close to the absorption edge, where the structure is subject to weak fluctuations due to the absorption of photon energy. When bombarded by photons of higher energies than the ionization energy, core-electrons will eject as photoelectrons, as in XPS[75], leading to core-holes in the K shell. Two distinct relaxation mechanisms may occur, which involve annihilation of the mentioned core-hole, one resulting in emission of fluorescence while the other ends in a final state consisting of two electron-holes. The latter phenomena is known as the Auger-effect, where an electron de-excites to the K shell transferring the additional energy to another electron, which thereby leaves the molecule and is then called an

Auger-electron. However, when the molecule is exposed to hard X-rays, the de-excitation of an electron to the K shell results in emission of energy, known as fluorescence. Both of these mechanisms are measured by the EXAFS technique, extended X-ray absorption fine structure[75].

XPS and NEXAFS provide description of the electronic structure of atoms or molecules by construction of emission and absorption spectra, however, these experimental techniques are expensive in use and theoretical spectra are therefore of great value. In addition, theoretical spectra have proven as a helpful tool for interpretation of experimental spectra[76–78].

4. Method

Consider the ionization process described in the previous chapter, namely excitation of core-electrons to a super-diffuse orbital that is included in the basis set. Employing this approach for core-ionization together with the EOM-CC framework and the CVS technique, results in a model for core-ionization energies. Restriction of the triple projection manifold such that the core excitations to the diffuse orbital are the only excitations taken into account, leads to a decrease in computational cost when compared to EOM-CCSDT, as the scaling of EOM-CCSDT is the same as for CCSDT. Furthermore, the level of accuracy of the proposed model remains close to the accuracy of CCSDT. Thus, the computational cost is reduced with respect to EOM-CCSDT, while the accuracy of the model is at level with the accuracy of CCSDT, two factors that lay the foundation of a promising model. The model is called XPS-CCSD since the experimental equivalent is the process occurring in XPS, as mentioned in Chapter 3.1.

In order to only include the triple excitations involving the specific core excitation, the triple cluster operator is a summation only over two virtual and two occupied orbitals. The initial core orbital, denoted I, and the final super diffuse orbital, denoted A, are thus considered as fixed molecular orbitals. A restricted projection manifold is utilised, where the single and double projection manifolds are included in their completeness, while the triple projection manifold is restricted as mentioned.

The XPS-CCSD model constitutes a Jacobian matrix where the triple excitation operator, $\hat{\tau}_{\nu_3}^{\text{XPS}}$, includes the two terms $\hat{\tau}_{\nu_3}^{(1)}$ and $\hat{\tau}_{\nu_3}^{(2)}$. These triple excitation operators are given as

$$\hat{\tau}_{AIbjck}^{(1)} = E_{AI}E_{bj}E_{ck}, \tag{24}$$

$$\hat{\tau}_{AjbIck}^{(2)} = E_{Aj}E_{bI}E_{ck}. \tag{25}$$

In comparison, the CCSDT Jacobian matrix, see Matrix (23) in Chapter 2.3, includes the full triple cluster operator, $\hat{T}_3$, with the corresponding triple excitation operator $\hat{\tau}_{\nu_3}$. The Jacobian matrix for the XPS-CCSD model may be written as

$$\mathbf{A}^{\mathrm{XPS}} = \begin{pmatrix} \langle\mu_1|\,[\hat{H}^T,\hat{\tau}_{\nu_1}]\,|\mathrm{HF}\rangle & \langle\mu_1|\,[\hat{H}^T,\hat{\tau}_{\nu_2}]\,|\mathrm{HF}\rangle & \langle\mu_1|\,[\hat{H}^T,\hat{\tau}^{\mathrm{XPS}}_{\nu_3}]\,|\mathrm{HF}\rangle \\ \langle\mu_2|\,[\hat{H}^T,\hat{\tau}_{\nu_1}]\,|\mathrm{HF}\rangle & \langle\mu_2|\,[\hat{H}^T,\hat{\tau}_{\nu_2}]\,|\mathrm{HF}\rangle & \langle\mu_2|\,[\hat{H}^T,\hat{\tau}^{\mathrm{XPS}}_{\nu_3}]\,|\mathrm{HF}\rangle \\ \langle\mu^{\mathrm{XPS}}_3|\,[\hat{H}^T,\hat{\tau}_{\nu_1}]\,|\mathrm{HF}\rangle & \langle\mu^{\mathrm{XPS}}_3|\,[\hat{H}^T,\hat{\tau}_{\nu_2}]\,|\mathrm{HF}\rangle & \langle\mu^{\mathrm{XPS}}_3|\,[\hat{H}^T,\hat{\tau}^{\mathrm{XPS}}_{\nu_3}]\,|\mathrm{HF}\rangle \end{pmatrix}, \quad (26)$$

where $\left\langle\mu^{\mathrm{XPS}}_3\right|$ denotes the triple projection manifold only involving excitations from core orbital I to the super-diffuse orbital A, and consists of the states $\left\{\left\langle \substack{Abc\\Ijk}\right|\right\}$ and $\left\{\left\langle \substack{Abc\\jIk}\right|\right\}$. Note that the elements belonging to the CCSD part of this matrix will be equal to the CCSD Jacobian matrix, see Matrix (22). The triple excitations will not give a contribution to the ground state as

$$\left\langle\mu^{\mathrm{XPS}}_3\right|\hat{H}^{\mathrm{T}}\left|\mathrm{HF}\right\rangle = 0,$$

since all the triple excitation amplitudes are equal to zero, $t^{\mathrm{XPS}} = 0$, due to the final state containing $N-1$ electrons, which is one less electron than the ground state. That the above equation is equal to zero is a criteria for the EOM-CC model to work properly, see Chapter 2.3. The cluster operator is truncated after the second term in the XPS-CCSD model, as is the case for CCSD, but the cluster operator may be seen as $\hat{T} = \hat{T}_1 + \hat{T}_2 + \hat{T}^{\mathrm{XPS}}$, where the triple cluster operator is equal to zero due to that the triple excitation amplitudes are equal to zero. However, note that the triple excitation operator $\hat{\tau}^{\mathrm{XPS}}_{\nu_3}$ is present in the elements of the XPS-CCSD Jacobian matrix.

Biorthogonality is obtained from the overlap integrals

$$\begin{aligned} \left\langle \substack{\overline{a}\\i}\,\middle|\,\substack{c\\k}\right\rangle &= \delta_{ai,ck}, \\ \left\langle \substack{\overline{ab}\\ij}\,\middle|\,\substack{cd\\kl}\right\rangle &= P^{cd}_{kl}\delta_{ai,ck}\delta_{bj,dl} = P^{ab}_{ij}\delta_{ai,ck}\delta_{bj,dl}, \\ \left\langle \substack{\overline{abc}\\ijk}\,\middle|\,\substack{def\\lmn}\right\rangle &= P^{abc}_{ijk}\delta_{ai,dl}\delta_{bj,em}\delta_{ck,fn}, \end{aligned}$$

where the biorthogonal bra states are denoted with an overbar. P^{ab}_{ij} denotes the double permutation operator and P^{abc}_{ijk} the triple permutation operator, which, respectively, induces six states for the triple projection manifold and two states for the double projection manifold, as follows

$$P_{ij}^{ab} A_{ij}^{ab} = A_{ij}^{ab} + A_{ji}^{ba}, \tag{27}$$

$$P_{ijk}^{abc} A_{ijk}^{abc} = A_{ijk}^{abc} + A_{ikj}^{acb} + A_{jik}^{bac} + A_{jki}^{bca} + A_{kij}^{cab} + A_{kji}^{cba}. \tag{28}$$

Where A_{ij}^{ab} and A_{ijk}^{abc} denote general integrals. From the biorthogonal states, the double projection manifold of the biorthonormal states may be written as

$$\left\langle \widetilde{\substack{ab \\ ij}} \right| = \frac{1}{1 + \delta_{ai,bj}} \left\langle \overline{\substack{ab \\ ij}} \right| = \frac{1}{\Delta_{aibj}} \left\langle \overline{\substack{ab \\ ij}} \right|,$$

where the tilde denotes the biorthonormal bra-state. Likewise, the biorthonormal basis for the triple case yields

$$\left\langle \widetilde{\substack{abc \\ ijk}} \right| = \frac{1}{1 + \delta_{ai,bj} + \delta_{ai,ck} + \delta_{bj,ck}} \left\langle \overline{\substack{abc \\ ijk}} \right| = N_{ijk}^{abc} \left\langle \overline{\substack{abc \\ ijk}} \right|.$$

In order to solve the eigenvalue problem, see Equations (20) and (21), a linear transformation is performed where the coefficients are given as column vectors and written as

$$\mathbf{c} = \mathbf{c_1} + \mathbf{c_2} + \mathbf{c_3}^{(1)} + \mathbf{c_3}^{(2)} = \begin{pmatrix} c_1 \\ 0 \\ 0 \\ 0 \end{pmatrix} + \begin{pmatrix} 0 \\ c_2 \\ 0 \\ 0 \end{pmatrix} + \begin{pmatrix} 0 \\ 0 \\ c_3^{(1)} \\ 0 \end{pmatrix} + \begin{pmatrix} 0 \\ 0 \\ 0 \\ c_3^{(2)} \end{pmatrix} = \begin{pmatrix} c_1 \\ c_2 \\ c_3^{(1)} \\ c_3^{(2)} \end{pmatrix}.$$

The linear transformed system is denoted as σ, and has the form

$$\begin{aligned} \sigma = \mathbf{A}^{\mathrm{XPS}}\mathbf{c} &= \mathbf{A}^{\mathrm{XPS}}\mathbf{c_1} + \mathbf{A}^{\mathrm{XPS}}\mathbf{c_2} + \mathbf{A}^{\mathrm{XPS}}\mathbf{c_3}^{(1)} + \mathbf{A}^{\mathrm{XPS}}\mathbf{c_3}^{(2)} \\ &= \sigma_1 + \sigma_2 + \sigma_3, \end{aligned} \tag{29}$$

where

$$\sigma_\gamma = \sigma_{\gamma,ai} + \sigma_{\gamma,aibj} + \sigma_{\gamma,aibjck}, \qquad \gamma = 1, 2 \tag{30}$$

$$\begin{aligned} \sigma_3 &= \sigma_{3,ai} + \sigma_{3,aibj} + \sigma_{3,aibjck} \\ &= \rho_{3,ai}^{(1)} + \rho_{3,ai}^{(2)} + \rho_{3,aibj}^{(1)} + \rho_{3,aibj}^{(2)} + \rho_{3,aibjck}^{(1)} + \rho_{3,aibjck}^{(2)}. \end{aligned} \tag{31}$$

Notation-wise, the terms belonging to triple excitations are further divided into two terms, designated as $\rho^{(1)}_{3,\dots}$ and $\rho^{(2)}_{3,\dots}$, as observed above. Note that for terms emerging from $\hat{\tau}^{(2)}_{\nu_3}$ there is a loss of symmetry for the linear transformation coefficients, as mentioned in Appendix G. In other words, $C^{AI}_{bj,ck} = C^{AI}_{ck,bj}$, but $B^{AI}_{b,j,dl} \neq B^{AI}_{d,l,bj}$, thereby the $c^{(1)}_3$-coefficients consist of a symmetric matrix, while the $c^{(2)}_3$-coefficients consist of a non-symmetric matrix. This non-symmetry of the $B^{AI}_{b,j,dl}$ is also emphasized in the notation by the two commas in the subscript. The superscript of a matrix element denotes the fixed orbitals, for instance the fixed orbitals for $B^{aj}_{b,i,dl}$ are a and j.

Expressions for $\sigma_{1,aibjck}$, $\sigma_{2,aibjck}$ and $\sigma_{3,aibjck}$ were derived in accordance with the procedure given in Appendix E, and the final expressions are presented in Appendix F. Note that the triple projection manifold is written on the general form in the following expressions for $\sigma_{1,aibjck}$, $\sigma_{2,aibjck}$ and $\sigma_{3,aibjck}$. In other words, the triple projection manifold is not yet restricted to only involving the specific core excitation. In addition, the two-electron integrals, the contracted two-integrals and the elements of the inactive Fock matrix are written without tilde even though they are $\hat{T}_1$-transformed.

4.1. Difference from EOM-CCSD and EOM-CCSDT. Considering the modifications mentioned above, the difference of XPS-CCSD when compared to EOM-CCSDT is the restriction of the triple projection manifold and the truncation level of the cluster operator. The XPS-CCSD model includes excitations of a higher level than CCSD, but not all excitations included in CCSDT are present. This feature results in more cumbersome expressions than what is the case for the EOM-CCSD model, however, when compared to EOM-CCSDT the expressions are not as numerous. Application of the CVS technique ensures that core excitations are the only ones taken into account, while further restriction of the triple excitations results in that *only* core excitations to the super-diffuse orbital are occurring. In addition, note that the ground state triple excitation amplitudes are equal to zero, $t^{Abc}_{Ijk} = t^{Abc}_{jIk} = 0$, due to the ionized state containing $N-1$ electrons, while the ground state is containing N electrons. Such that the $N-1$-state is not represented in the Slater determinants included in the ground state wave function.

Furthermore, the cluster operator is truncated after the second term, not the third as is done in the EOM-CCSDT model. However, a zero contribution is added to the truncated cluster operator, representing the triple cluster operator.

Note that the two triple excitation operators $\hat{\tau}_{\nu_3}^{(1)}$ and $\hat{\tau}_{\nu_3}^{(2)}$ in the XPS-CCSD Jacobian matrix, see Matrix (26), still contribute even though the triple cluster operator is equal to zero, accordingly including a higher level of electron interactions than what is the case for CCSD.

4.2. The super-diffuse orbital. As proposed by Stanton and Gauss, an orbital with super-diffuse character is included in the basis set [46], more precisely, the super-diffuse orbital is included in the set of virtual molecular orbitals. The exponent of a Gaussian basis function added to the basis set is set to nearly zero. In this manner the super-diffuse orbital has no interactions with the molecular or atomic orbitals, which is warranted in order to describe an ionization process.

For a more general treatment, bath-orbitals may be used. Introduction of such orbitals means to add orbitals that do not interact with the molecular orbitals and all integrals involving such bath-orbitals are explicitly set to zero. In this manner, instabilities regarding the integral code that can arise from very small orbital exponents are avoided.

5. Implementation

Final expressions of the linear transformed XPS-CCSD Jacobian matrix, see Equation (29) and Matrix (26), are given in Appendix F. These expressions, except the expressions corresponding to the CCSD Jacobian matrix, see Matrix (22), were implemented in a coupled cluster program developed at the quantum chemistry group at NTNU. The pilot code is object oriented and was implemented using Fortran 2008. Expressions for $\sigma_{1,ai}$, $\sigma_{1,aibj}$, $\sigma_{2,ai}$ and $\sigma_{2,aibjck}$ in Appendix F are not included in the implementation of the linear transformed XPS-CCSD Jacobian, as the XPS-CCSD class inherits from the already implemented CCSD class. All together the submodule containing the XPS-CCSD-expressions contains over 20 000 lines of code.

The expressions were implemented as they appear in Appendix F, meaning that the triple permutation operator was not unwrapped in the implemented terms, but applied afterwards. As a consequence, every possible term was calculated, also the ones not involving a core-ionization. However, only the terms belonging to the mentioned projection manifold were allowed to contribute to the sigma vectors. In that manner, the projection manifold was restricted.

Terms involving integrals with the diffuse orbital are equal to zero, since the diffuse orbital does not interact with any of the other molecular orbitals, as mentioned in Chapter 4.2. For instance, the terms including g_{mAld}, which belongs to $\rho^{(2)}_{3,aibjck}$, or L_{bdlA}, which belongs to $\rho^{(2)}_{3,aibj}$, are all equal to zero. Both of the mentioned expressions are given in Appendix F.

5.1. Debugging.

An EOM-CCSDT calculation where the ground state triple excitation amplitudes were set equal to zero was performed by Dr. Devin A. Matthews at University of Texas in Austin. Hence, the CCSD wave function was used as the ground state function and the truncation level of the cluster operator is the same as what is used in the XPS-CCSD model. In addition, all excitations not involving the specific core excitation to the super-diffuse orbital were neglected. In this manner, the CCSDT-calculation takes the same excitations as the XPS-CCSD model into account, and the results obtained by these two models should therefore be equal.

Dr. Matthews's calculations proved useful in debugging the pilot code, since the obtained result was compared to the corresponding result obtained by Dr.

Matthews. Note that since a CCSDT calculation was performed, the computational cost corresponded to a scaling of n^8, while XPS-CCSD currently scales as n^7.

The coefficient matrices for the triple excitations, $C^{AI}_{bj,ck}$ and $B^{AI}_{b,j,ck}$, contain some of the same elements. As a consequence, linear dependence emerged and the result became equal to zero. This problem was explicitly handled in the code.

5.2. Computational Cost. The XPS-CCSD model scales as n^7, but would scale as n^6 if only the terms belonging to the restricted projection manifold were calculated, which could be done by writing out all the terms emerging when operating the triple permutation operator, P^{abc}_{ijk}, and only including the relevant terms. Relevant terms are in this case terms that involve the core-ionization. This was not done due to the amount of work and limitation of time, as the triple permutation operator leads to six terms for each term and both $\rho^{(1)}_{3,aibjck}$ and $\rho^{(2)}_{3,aibjck}$ already consist of numerous terms.

Although the scaling of the XPS-CCSD model, when only including terms as described above, is n^6, the approach may lead to greater computational cost than EOM-CCSD, which also scales as n^6. The most expensive contribution in the EOM-CCSD model scales as $n^2_{\mathrm{occ}} n^4_{\mathrm{vir}}$ [26], n_{occ} denoting the number of occupied orbitals and n_{vir} denoting the number of virtual orbitals, while the most expensive contribution in the XPS-CCSD model may involve a greater power of the number of virtual orbitals. In addition, depending on the ratio between n_{occ} and n_{vir} there might be several terms that deserve the name "the most expensive contribution", while in EOM-CCSD there is only one term scaling as $n^2_{\mathrm{occ}} n^4_{\mathrm{vir}}$.

6. Preliminary Results

Table 3 displays core-ionization energies for H_2O, CO and NH_3 obtained using the coupled cluster methods CCSD, CC(2,3), XPS-CCSD, CCSD(T)(a) and CCSDT for different basis sets. The discrepancies from the CCSDT-energies when compared to energies obtained by CCSD, CC(2,3), XPS-CCSD and CCSD(T)(a) are noted in the columns named ΔCCSD, ΔXPS-CCSD and ΔCCSD(T)(a), respectively. CC(2,3) denotes the modified CCSDT-calculation performed by Dr. Matthews, as mentioned in Chapter 5.1.

The augmented correlation-consistent polarized core-valence set, aug-cc-pCVXZ, of Woon and Dunning[79] was utilized for all four molecules, where the triple zeta and quadruple zeta sets were applied. Inclusion of core, core-valence and valence correlations are represented by the core-valence part of the basis set, where core correlations are important for describing core excitations properly.

Note that the column named ΔCCSD contains the greatest energy differences, which is in accordance with the accuracy of the model when compared to the other models presented in the table. Compared to models that includes triple contributions, CCSD takes less electron interactions into account and therefore provides a poorer description of the electronic structure.

In addition, large orbital relaxation effects will occur due to promotion of core-electrons since the screening effect of the nucleus weakens[71;80;81]. These effects will not be described sufficiently by only double excitations, as excitation of one of the electrons is saved for promotion of a core-electron to the diffuse orbital. Thus, in order to properly describe the orbital relaxation, at least triple excitations are needed.

As observed in Table 3, the values of CC(2,3) and XPS-CCSD differ, which is most apparent, when considering energies obtained by using basis set aug-cc-pCVTZ, for CO when the excited core-orbital belongs to oxygen. These energies differ by 0.0003121 eV, as observed in Table A.1 in Appendix A where the deviations of these two calculations are given. Comparison of the rest of the energies for the same basis set, prove a difference in the fourth decimal, a deviation of magnitude close to 10^{-4} eV, where the XPS-CCSD energies are greatest in each case. This implies that the XPS-CCSD pilot code still contains some minor errors, as the CC(2,3) model and the XPS-CCSD model should produce the same energies.

TABLE 3. Comparison of core-ionization energies of different coupled cluster models within the basis sets aug-cc-pCVTZ and aug-cc-pCVQZ for molecules H_2O, CO and NH_3. For CO, core-ionizations originating from both atoms are noted. In the column named CC(2,3) energies of a modified CCSDT model are noted, here the triple amplitudes are set equal to zero while the CCSD-state is used as the ground state, thus the model resembles the XPS-CCSD model and will provide equal energies. The energy differences between CCSDT and the other models are noted in columns named ΔCCSD, ΔCC(2,3), ΔXPS-CCSD and ΔCCSD(T). Energies are given in eV. Pilot calculations for CC(2,3) were performed by Dr. Devin A. Matthews at University of Texas in Austin, and he has provided the other numbers as well, except for the CCSDT energies which are due to Lan Chang at Johns Hopkins.

Basis set	Molecule	CCSD	CC(2,3)	XPS-CCSD*	CCSD(T)(a)	CCSDT	ΔCCSD	ΔCC(2,3)	ΔXPS-CCSD	ΔCCSD(T)(a)
	H_2O									
aug-cc-pCVTZ		541.477	539.389	539.389	539.622	539.612	1.865	0.224	0.223	0.010
aug-cc-pCVQZ		541.403	539.220	539.196	539.480	539.464	1.939	0.245	0.268	0.015
	CO (C)									
aug-cc-pCVTZ		297.620	296.170	296.170	296.567	296.431	1.189	0.262	0.261	0.136
aug-cc-pCVQZ		297.613	296.095	296.086	296.502	296.361	1.251	0.266	0.276	0.141
	CO (O)									
aug-cc-pCVTZ		544.269	541.985	541.986	542.212	542.255	2.015	0.269	0.269	0.043
aug-cc-pCVQZ		544.206	541.834	541.819	542.085	542.123	2.083	0.289	0.304	0.038
	NH_3									
aug-cc-pCVTZ		407.031	405.244	405.244	405.493	405.466	1.565	0.222	0.222	0.027
aug-cc-pCVQZ		406.985	405.102	405.074	405.375	405.342	1.643	0.239	0.267	0.033

*Note that the XPS-CCSD energies are not equal to the corresponding CC(2,3)energies, meaning the pilot XPS-CCSD code still contains minor errors.

In addition, it appears that the error increases with increasing basis set size, as observed in Table A.1. For energies given in Table 3, the three decimals included for the XPS-CCSD ionization energy for H_2O, for instance, in the aug-cc-pCVQZ basis set differs from the corresponding CC(2,3) energy. Meanwhile, the error is not visible for the decimals included for the aug-cc-pCVTZ basis set, and values in Table A.1 proves that the error is close to a magnitude of 10^{-2} eV for the aug-cc-pCVQZ basis set. Notice that the XPS-CCSD energies are greater than the CC(2,3) energies when the aug-cc-pCVTZ basis set is utilized, while the energies obtained by XPS-CCSD are of less magnitude than the CC(2,3) energies for the aug-cc-pCVQZ basis set. Such an error increase may suggest that a summation over the virtual orbitals is erroneously truncated.

Inclusion of triple excitations in the XPS-CCSD model results in core-ionization energies closer to experimental values than the EOM-CCSD model provides, as observed in Tables 2 and 3. This is to be expected due to the level of excitations included in the CCSD model and the large orbital relaxation effects that emerges, as mentioned previously. In addition, in order to obtain accurate ionization energies it has been proven that the CCSD-level does not suffice, as the inclusion of triple contributions usually decrease the CCSD ionization energies[67]. All together, it is safe to say that inclusion of triple excitations improves the core-ionization energies.

The CCSD(T)(a) approach provides core-ionization energies closest to the CCSDT-energies, as observed in Table 3, as the values of the ΔCCSD(T)(a)-column clearly are of the smallest magnitude compared to the other columns containing discrepancies. As for XPS-CCSD-calculations, the computational cost of CCSD(T)(a)-calculations corresponds to a scaling of n^7, but remember that the cost of the XPS-CCSD model could be reduced to n^6.

As observed in Table 3, the ionization energies obtained by the XPS-CCSD model are close to the CCSDT-energies, as the deviations are in the range of 0.222-0.304 eV. Even though the level of electron interactions included in the model is not as high as for what is included in CCSDT, the interactions which contribute significantly to the core-ionization energy are taken into account. The XPS-CCSD model thus performs at a level of accuracy comparable to CCSDT, which was expected due to the inclusion of significant excitations.

Values in the column named ΔXPS-CCSD are of equal magnitude; approximately 0.2-0.3 eV, and for the basis set aug-cc-pCVTZ the difference from

CCSDT is approximately 0.222-0.269 eV, while for the aug-cc-pCVQZ the difference is larger, approximately 0.267-0.304 eV. Further calculations on other molecules may prove that the deviation will remain within these intervals. In that case, the model might prove to be a useful tool for estimating CCSDT core-ionization energies, as XPS-CCSD-calculations have lower computational cost than CCSDT-calculations. That the deviation from CCSDT increases with basis set size might be that there are less electron interactions included in the model than what the case is for CCSDT, such that the following error enlarges when the system is more accurately described.

Comparing the XPS-CCSD model and the CCSDT model, the advantage of XPS-CCSD is the reduction in computational cost. Although the accuracy is reduced as well, the reduction of the computational cost triumphs the loss of accuracy. When the computational cost is decreased, the model can be applied on larger systems that are too large for the CCSDT model to be practical.

Coriani and Koch calculated core-ionization energies by applying the CVS technique within the EOM-CCSD framework and restrict the core excitations to only involving excitation to a super-diffuse orbital[45]. The obtained core-ionization energies proved to be in line with previous findings, which confirmed the validity of the approach for obtaining core-ionization energies.

The CVS approach is also an approximation which affects the accuracy of the results. However, as stated by Coriani and Koch, this approach has proved as an accurate approximation, where the excitation energies differ by less than 0.05 eV when compared to application of the full Lanczos algorithm[45]. Furthermore, Myhre *et al.* constructed theoretical NEXAFS spectra for ethanal, propenal and butanal where both the Lanczos algorithm and the Davidson algorithm with the CVS approximation were applied, and the error due to the CVS approximation remained minor in all cases[71]. Similarly, when applying the CVS approximation with the CC3 model[72], the error remained small. In conclusion, even though application of the CVS technique does induce errors, the approximation is valid when calculating core-ionization energies as the errors are non-significant.

Finally, note that the XPS-CCSD model is an EOM-CC model, such that the properties of EOM-CC models apply, see Chapter 2.3.

7. Concluding remarks and further work

Introducing a super-diffuse orbital in the basis set and making use of the CVS technique within the EOM-CC framework results in a model for core-ionization energies. Further restriction of triple excitations to only include states corresponding to core excitations to the super-diffuse orbital leads to a model involving a higher degree of electron interactions than CCSD, but not as high as a full CCSDT model. Note that the truncation level of the cluster operator remains as in CCSD. The model corresponds to the experimental XPS process and it is not a full CCSDT model, thereof the name XPS-CCSD.

Expressions of the linear transformed Jacobian matrix for the XPS-CCSD model were derived and implemented. Preliminary testing of the pilot code was performed on H_2O, CO and NH_3 for the two basis sets aug-cc-pCVTZ and aug-cc-pCVQZ. Comparison of the obtained results with results of a modified CCSDT calculation proved that the pilot code still contains minor errors. The modification of the CCSDT calculation involved neglecting all excitations not corresponding to promotion of a core electron to the super-diffuse orbital, such that the XPS-CCSD model and the modified CCSD-calculation should produce equal core-ionization energies. Further work includes debugging the pilot code and eliminate all errors such that the modified CCSDT calculations and the XPS-CCSD model produce exactly the same results. In addition, the pilot code could become more efficient by evaluation of the structure and contraction choices.

The XPS-CCSD model scales as n^7, but the scaling could be further reduced to n^6 by writing out the emerging terms when the permutation operator is applied and only including the terms involving core excitation to the super-diffuse orbital in the model. Note, however, that the most expensive terms might be numerous and of a greater power of the number of virtual orbitals than what is the case for CCSD.

Calculated core-ionization energies for H_2O, CO and NH_3 obtained by a bug-free XPS-CCSD calculation differ from energies obtained by CCSDT by 0.22-0.29 eV. These discrepancies are a result of a comparison of the modified CCSDT model with the full CCSDT model. Thus, the accuracy of the proposed model is at level with CCSDT. The great advantage of the model, however, is this level of accuracy combined with a possibility of a computational cost corresponding to a scaling of n^6. This factor widens the range of the selection of molecules

where the model is applicable, the selection now consisting of larger molecules than what the case is for CCSDT calculations.

Further testing of the XPS-CCSD model when applied to a range of molecules may prove that the model can be used as an estimation for CCSDT core-ionization energies, if the discrepancies between CCSDT calculations and XPS-CCSD calculation remains within the specific range. There should also be further testing with different basis sets in order to outline how the model behaves and how large basis sets that are needed for a proper description.

The combination of the accuracy and the computational cost of n^7, which could be reduced to n^6, makes the proposed model a well functioning and promising model for core-ionization energies.

Bibliography

[1] E. Schrödinger. An undulatory theory of the mechanics of atoms and molecules. *Phys. Rev.*, 28:1049–1070, 1926.

[2] J.A. Pople. Nobel lecture: Quantum chemical models. *Rev. Modern Phys.*, 71:1267–1274, 1999.

[3] O. Sinanoglu. Many-electron theory of atoms and molecules. I. Shells, electron pairs vs many-electron correlations. *J. Chem. Phys.*, 36:706–717, 1962.

[4] F. Coester and H. Kümmel. Short-range correlations in nuclear wave functions. *Nuc. Phys.*, 17:477–485, 1960.

[5] J. Čížek. On the correlation problem in atomic and molecular systems. calculation of wave function components in Ursell-type expansion using quantum-field theoretical methods. *J. Chem. Phys.*, 45:4256–4266, 1966.

[6] J. Paldus, J. Čížek, and I. Shavitt. Correlation problems in atomic and molecular systems. Extended coupled-pair many-electron theory and its application to the BH_3 molecule. *Phys. Rev.*, 5:50–67, 1972.

[7] R.J. Bartlett. Coupled-cluster approach to molecular structure and spectra: A step toward predictive quantum chemistry. *J. Phys. Chem.*, 93:1697–1708, 1989.

[8] R.J. Bartlett and M. Musial. Coupled cluster theory in quantum chemistry. *Rev. Mod. Phys.*, 79:291, 2007.

[9] G. Scuseria, C. L. Janssen, and H. F. Schaefer. The closed-shell coupled cluster single and double excitation (CCSD) model for the description of electron correlation. A comparison with the configuration interaction (CISD) results. *J. Chem. Phys*, 86:2881–2890, 1988.

[10] G. D. Purvis and R. J. Bartlett. A full coupled-cluster singles and doubles model: The inclusion of disconnected triples. *J. Chem. Phys*, 76:1910–1918, 1982.

[11] G. E. Scuseria, C. L. Janssen, and H. F. Schaefer. An efficient reformulation of the closed-shell coupled cluster single and double excitation (CCSD) equations. *J. Chem. Phys*, 89:7382–7387, 1988.

[12] J. Noga and R. J. Bartlett. The full CCSDT model for molecular electronic structure. *J. Chem. Phys*, 86:7041–7050, 1987.

[13] H. Koch, O. Christiansen, P. Jørgensen, and J. Olsen. Excitation energies of BH, CH_2 and Ne in full configuration interaction and the hierarchy CCS, CC2, CCSD and CC3 of coupled cluster models. *Chem. Phys. Letters*,

244:75–82, 1995.

[14] H. Koch, O. Christiansen, P. Jørgensen, A.M. Sanchez de Merás, and T. Helgaker. The CC3 model: An iterative coupled cluster approach including connected triples. *J. Chem. Phys.*, 106:1808, 1996.

[15] K. Raghavachari, G. Trucks, J. A. Pople, and M. Head-Gordon. A fifth-order perturbation comparison of electron correlation theories. *Chem. Phys. Letters*, 157:479–483, 1989.

[16] Y. S. Lee, S. A. Kucharski, and R.J. Bartlett. A coupled cluster approach with triple excitations. *J. Chem. Phys.*, 81:5906–5912, 1984.

[17] M. Urban, J. Noga, S. J. Cole, and R. J. Bartlett. Towards a full CCSDT model for electron correlation. *J. Chem. Phys.*, 83:4041–4046, 1985.

[18] S. A. Kucharski and R. J. Bartlett. Coupled-cluster methods that include connected quadruple excitations, T_4: CCSDTQ-1 and Q(CCSDT)*. *Chem. Phys. Letters*, 58:550–555, 1989.

[19] M Musial, S. A. Kucharski, and R. J. Bartlett. T_5 operator in coupled cluster calculations. *Chem. Phys. Letters*, 320:542–548, 2000.

[20] M Musial, S. A. Kucharski, and R. J. Bartlett. Formulation and implementation of the full coupled-cluster method through pentuple excitations. *J. Chem. Phys.*, 116:4382–4288, 2002.

[21] J. Čížek. Origins of coupled cluster technique for atoms and molecules. *Theor. Chim. Acta*, 80:91–94, 1991.

[22] T. Helgaker, P. Jørgensen, and J. Olsen. *Molecular Electronic-Structure Theory*, chapter 7, pages 256–286. John Wiley & Sons, Ltd, 2000.

[23] D. I. Lyakh, M. Musial, V. F. Lotrich, and R. J. Bartlett. Multireference nature of chemistry: The coupled-cluster view. *Chem. Rev.*, 112:183–243, 2012.

[24] S. A. Kucharski, A. Balková, P. G. Szalay, and R. J. Bartlett. Hilbert space multireference coupled-cluster methods. II. A model study on H_8. *J. Chem. Phys.*, 97:4289–4300, 1992.

[25] P. Atkins and R. Friedman. *Molecular Quantum Mechanics*, chapter 9, pages 295–337. Oxford University Press, 5$^{\text{th}}$ edition, 2011.

[26] T. Helgaker, P. Jørgensen, and J. Olsen. *Molecular Electronic-Structure Theory*, chapter 13, pages 648–723. John Wiley & Sons, Ltd, 2000.

[27] T. Helgaker, P. Jørgensen, and J. Olsen. *Molecular Electronic-Structure Theory*, chapter 14, pages 724–816. John Wiley & Sons, Ltd, 2000.

[28] H. J. Monkhorst. Calculation of properties with the coupled-cluster method. *Intern. J. Quantum Chem. Symp.*, 11:421–432, 1977.

[29] K. Emrich. An extension of the coupled cluster formalism to excited states. *Nucl. Phys. A*, 351:379–396, 1981.

[30] H. Sekino and R. J. Bartlett. A linear response, coupled-cluster theory for excitation energy. *Intern. J. Quantum Chem. Symp.*, 18:255–265, 1984.

[31] J.F. Stanton and R.J. Bartlett. The equation of motion coupled cluster method. A systematic biorthogonal approach to molecular excitation energies, transition probabilities. *J. Chem. Phys.*, 98:7029–7039, 1993.

[32] S. A. Kucharski, M. Wloch, M. Musial, and R. J. Bartlett. Coupled-cluster theory for excited electronic states: The full equation-of-motion coupled-cluster single, double, and triple excitation method. *J. Chem. Phys.*, 115:8263–8266, 2001.

[33] J. Geerstsen, M. Rittby, and R.J. Bartlett. The equation-of-motion coupled cluster method: Excitation energies of Be and CO. *Chem. Phys. Letters*, 164:57–62, 1989.

[34] D. Comeau and R. J. Bartlett. The equation-of-motion coupled-cluster approach. Applications to open- and closed-shell reference states. *Chem. Phys. Letters*, 207:414–423, 1993.

[35] M. Nooijen and R. J. Bartlett. Similarity transformed equation-of-motion coupled-cluster theory: Details, examples and comparisons. *J. Chem. Phys.*, 107:6812–6830, 1997.

[36] K. Kowalski and P. Piecuch. The active-space equation-of-motion coupled-cluster methods for excited states: The EOMCCSDt approach. *J. Chem. Phys.*, 113:8490–8502, 2000.

[37] H. Koch, H. J. Aa. Jensen, P. Jørgensen, and T. Helgaker. Excitation energies from the coupled cluster singles and doubles linear response function (CCSDLR). Application to Be, CH^+, CO and H_2O. *J. Chem. Phys.*, 93:3345–3350, 1990.

[38] T. Bondo Pedersen and H. Koch. Coupled cluster response functions revisited. *J. Chem. Phys.*, 106:8059–8072, 1997.

[39] H. Koch and P. Jørgensen. Coupled cluster response functions. *J. Chem. Phys.*, 93:3333–3344, 1990.

[40] R. Kobayashi, H. Koch, and P. Jørgensen. Calculation of frequency-dependent polarizabilities using coupled-cluster response theory. *Chem. Phys. Letters*, 219:30–35, 1994.

[41] H. Koch, R. Kobayashi, A. Sanchez de Merás, and P. Jørgensen. Calculation of size-intensive transition moments from the coupled cluster singles and doubles linear response function. *J. Chem. Phys.*, 100:4393–4400, 1994.

[42] M. Caricato, G. W. Trucks, and M. Frisch. On the difference between the transition properties calculated with linear response and equation of motion-CCSD approaches. *J. Chem. Phys.*, 131:174104:1–6, 2009.

[43] E. R. Davidson. The iterative calculation of a few of the lowest eigenvalues and corresponding eigenvectors of large real-symmetric matrices. *J. Comput. Phys.*, 17:87–94, 1975.

[44] C. Lanczos. An iteration method for the solution of the eigenvalue problem of linear differential and integral operators. *J. Research of the National Bureau of Standards*, 45:255–282, 1950.

[45] S. Coriani and H. Koch. Communication: X-ray absorption spectra and core-ionization potentials within a core-valence separated coupled cluster framework. *J. Chem. Phys.*, 143:181103:1–5, 2015.

[46] J.F. Stanton and J. Gauss. A simple scheme for the direct calculation of ionization potentials with coupled cluster theory that exploits established excitation energy methods. *J. Chem. Phys.*, 111:8785–8788, 1999.

[47] D. A. Matthews and J. F. Stanton. A new approach to approximate equaiton-of-motin coupled cluster with triple excitations. *J. Chem. Phys.*, 145:124102:1–15, 2016.

[48] A. A. Bakke, H. Chen, and W. L. Jolly. A table of absolute core-electron binding-energies for gaseous atoms and molecules. *J. Electron Spectroscopy and Related Phenomena*, 20:333–366, 1980.

[49] J. M. Hollas. *Modern Spectroscopy*, chapter 8, pages 289–336. John Wiley & Sons, Ltd, 4$^{\text{th}}$ edition, 2004.

[50] S. Coriani, T. Fransson, O. Christiansen, and P. Norman. Asymmetric-LANCZOS-chain-driven implementation of electronic resonance convergent coupled-cluster linear response theory. *J. Chem. Theory Comput.*, 8:1616–1628, 2012.

[51] S. Coriani, O. Christiansen, T. Fransson, and P. Norman. Coupled-cluster response theory for near-edge X-ray-absorption fine structure of atoms and molecules. *Phys. Rev.*, 85:022507:1–8, 2012.

[52] T. Fransson, S. Coriani, O. Christiansen, and P. Norman. Carbon X-ray absorption spectra of fluoroethenes and acetone: A study at the coupled cluster, density functional, and static-exchange leveles of theory. *J. Chem. Phys.*, 138:124311–124323, 2013.

[53] B. Peng, P. J. Lestrange, J. J. Goings, M. Caricato, and X. Li. Energy-specific equation-of-motion coupled-cluster methods for high-energy excited states: Application to K-edge X-ray absorption spectroscopy. *J.*

Chem. Theory Comput., 11:4146–4153, 2015.

[54] J. Brabec, K. Bhaskaran-Nair, N. Govind, J. Pittner, and K. Kowalski. Communication: Application of state-specific multireference coupled cluster methods to core-level excitations. *J. Chem. Phys.*, 137:171101–171104, 2012.

[55] J. Wenzel, M. Wormit, and A. Dreuw. Calculating core-level excitations and X-ray absorption spectra of medium-sized closed-shell molecules with the algebraic-diagrammatic construction scheme for the polarization propagator. *J. Comput. Chem.*, 35:1900–1915, 2014.

[56] T.J.A. Wolf, R.H. Myhre, J.P. Cryan, S. Coriani, R.J. Squibb, A. Battistoni, N. Berrah, C. Bostedt, P. Buckbaum, G. Coslovich, R. Feifel, K.J. Gaffney, J. Grilj, T.J. Martinez, S. Miyabe, S.P. Moeller, M. Mucke, R. Natan, A. Obaid, T. Osipov, O. Plekan, S. Wang, H. Koch, and M. Gühr. Probing ultrafast $\pi\pi^*/n\pi^*$ internal conversion in organic chromophores via K-edge resonant absorption. *Nature Communications*, 8:1–7, 2017.

[57] C. Jacoboni. *Theory of Electron Transport in Semiconductors*, chapter 23, pages 441–452. Springer, 2010.

[58] A. L. Fetter and J. D. Walecka. *Quantum Theory of Many-Particle Systems*, chapter 1, pages 3–32. Dover Publications, Inc., 1971 (2003).

[59] M. Doi. Second quantization representation for classical many-particle system. *J. Phys. A: Math. Gen.*, 9:1465–1477, 1976.

[60] P. Atkins and R. Friedman. *Molecular Quantum Mechanics*, chapter 7, pages 210–257. Oxford University Press, 5$^{\text{th}}$ edition, 2011.

[61] T. Helgaker, P. Jørgensen, and J. Olsen. *Molecular Electronic-Structure Theory*, chapter 1 and 2, pages 1–79. John Wiley & Sons, Ltd, 2000.

[62] T. Helgaker, S. Coriani, P. Jørgensen, K. Kristensen, J. Olsen, and K. Ruud. Recent advances in wave function-based methods of molecular-property calculations. *Chem. Rev.*, 112:543–631, 2012.

[63] H. Bruus and K. Flensberg. *Many-Body Quantum Theory in Condensed Matter Physics: An Introduction*, chapter 1, pages 1–30. Oxford University Press, 2004.

[64] J. F. Stanton and J. Gauss. Analytic energy derivatives for ionized states described by the equation-of-motion coupled cluster method. *J. Chem. Phys.*, 101:8938–8944, 1994.

[65] M. Musial and R. J. Bartlett. EOM-CCSDT study of the low-lying ionization potentials of ethylene, acetylene, and formaldehyde. *Chem. Phys.*

Letters, 384:210–214, 2003.

[66] R. Maitra, Y. Akinaga, and T. Nakajima. A coupled cluster theory with iterative inclusion of triple excitations and associated equation of motion formulation for excitation energy and ionization potential. *J. Chem. Phys.*, 147:074103:1–10, 2017.

[67] M. Musial, A. Kucharski, and R. J. Bartlett. Equation-of-motion coupled cluster method with full inclusion of the connected triple excitations for ionized states: IP-EOM-CCSDT. *J. Chem. Phys.*, 118:1128–1135, 2003.

[68] S. Hirata, M. Nooijen, and R. J. Bartlett. High-order determinantal equation-of-motion coupled-cluster calculations for ionized and electron-attached states. *Chem. Phys. Letters*, 328:459–468, 2000.

[69] M. Nooijen and R. J. Bartlett. Equation-of-motion coupled cluster method for electron attachment. *J. Chem. Phys.*, 102:3629–3647, 1995.

[70] M. Musial and R. J. Bartlett. Equation-of-motion coupled cluster method with full inclusion of connected triple excitations for electron-attached states: EA-EOM-CCSDT. *J. Chem. Phys.*, 119:1901–1908, 2003.

[71] R. H. Myhre, S. Coriani, and H. Koch. Near-edge X-ray absorption fine structure within multilevel coupled cluster theory. *J. Chem. Theory Comput.*, 12:2633–2643, 2016.

[72] R. H. Myhre, T. J. A. Wolf, L. Cheng, S. Nandi, S. Coriani, M. Gühr, and H. Koch. A theoretical and experimental benchmark study of core-excited states in nitrogen. *J. Chem. Phys.*, 148:064106:1–7, 2018.

[73] L. S. Cederbaum, W. Domcke, and J. Schirmer. Many-body theory of core holes. *Phys. Rev. A*, 22:206–222, 1980.

[74] D. C. Harris and M. D. Bertolucci. *Symmetry and Spectroscopy, An Introduction to Vibrational and Electronic Spectroscopy*, chapter 5, pages 307–419. Dover Publications, Inc, 1989 (1978).

[75] J. G. Chen. NEXAFS investigations of transition metal oxides, nitrides, carbides, sulfides and other interstitial compounds. *Surface Science Reports*, 30:1–152, 1997.

[76] O. Plekan, V. Feyer, R. Richter, M. Coreno, M. de Simone, K. C. Prince, A. B. Trofimov, E. V. Gromov, I. L. Zaytseva, and J. Schirmer. A theoretical and experimental study of the near edge X-ray absorption fine structure (NEXAFS) and X-ray photoelectron spectra (XPS) of nucleobases: Thymine and adenine. *Chem. Phys.*, 347:360–375, 2008.

[77] V. Feyer, O. Plekan, R. Richter, M. Coreno, M. de Simone, K. C. Prince, A. B. Trofimov, I. L. Zaytseva, and J. Schirmer. Tautomerism in cytosine

and uracil: A theoretical and expermential X-ray absorption and resonant Auger study. *J. Phys. Chem. A*, 114:10270–10276, 2010.

[78] T. Fransson, Y. Harada, N. Kosugi, N. A. Besley, B. Winter, J. J. Rehr, L. G. M. Petterson, and A. Nilsson. X-ray and electron spectroscopy of water. *Chem. Rev.*, 116:7551–7569, 2016.

[79] D. E. Woon and T. H. Dunning Jr. Gaussian basis for use in correlated molecular calculations. V. Core-valence basis sets for boron through neon. *J. Chem. Phys.*, 103:4572–4585, 1995.

[80] S. Sen, A. Shee, and D. Mukherjee. Inclusion of orbital relaxation and correlation through the unitary group adapted open shell coupled cluster theory using non-relativistic and scalar relativistic Hamiltonians to study the core ionization potential of molecules containing light to medium-heavy elements. *J. Chem. Phys.*, 148:054107:1–14, 2018.

[81] M Nooijen and R. J. Bartlett. Description of core-excitation spectra by the open-shell electron-attachment equation-of-motion coupled cluster method. *J. Chem. Phys.*, 102:6735–6756, 1995.

[82] T. Helgaker, P. Jørgensen, and J. Olsen. *Molecular Electronic-Structure Theory*, chapter 3, pages 80–106. John Wiley & Sons, Ltd, 2000.

List of symbols

Symbol	Definition	Description
N		Number of electrons
n		Number of basis functions
$\hat{T}$		Cluster operator
$\hat{T}_{n_i}$	$n_i = 1, 2, \ldots, N$, $i = 1, 2, \ldots, k$	n_i cluster operator
k	see Appendix D	Number of nested commutators
$\hat{H}$		Hamilton operator
Ψ		Wave function
E		Energy
M		Number of spin orbitals
P	$P = 1, \ldots, M$	General spin orbital
ϕ_P	$\phi_P(\mathbf{x}) = \phi_p(\mathbf{r})\sigma(m_s)$	Spin orbital number P
$\mathbf{x}$		Coordinate containing spatial and spin part
$\mathbf{r}$		Spatial coordinate
$\sigma(m_s)$		Spin function
m_s	$m_s = \alpha$ or β	Spin coordinate
α, β	$\frac{1}{2}$, $-\frac{1}{2}$ for fermions	Up or down spin
p, q, r, s		General orbitals
σ, τ		General spin functions
$\lvert\mathbf{k}\rangle$		Occupation number vector
k_P		Occupation number
$a_P^\dagger$	Equation (1)	Creation operator
δ_{ij}		Kronecker δ-function
$\Gamma_P^{\mathbf{k}}$		Phase factor
a_P	Equation (2)	Annihilation operator
E_{pq}	Equation (4)	Singlet excitation operator
e_{pqrs}	Equation (5)	Double excitation operator
h_{pq}	Equation (6)	One-integral
g_{pqrs}	Equation (7)	Two-integral
h_{nuc}	Equation (8)	Nuclear-repulsion
∇^2		Nabla operator squared
Z_I		Charge of nucleus I

Symbol	Definition	Description
r_I		Distance from an electron to nucleus I
r_{12}		Distance between electron 1 and 2
R_{IJ}		Separation between nucleus I and nucleus J
ψ_{nuc}		Nuclear wave function
ψ_{el}		Electronic wave function
$\|\text{CC}\rangle$		Coupled cluster wave function
$\|\text{HF}\rangle$		Hartree-Fock state
$\|\text{R}\rangle$		Reference state
$\hat{\tau}_\nu$		General excitation operator
t_ν		General excitation amplitude
$\|\mu\rangle$		General projection manifold
$\hat{H}^{\text{T}}$	$e^{-\hat{T}}\hat{H}e^{\hat{T}}$	Similarity transformed Hamiltonian
$\|\text{CCSD}\rangle$		CCSD wave function
t_{ij}^{ab}		double excitation amplitude
$a, b, c, \ldots$		Virtual orbitals
$i, j, k, \ldots$		Occupied orbitals
$\tilde{H}$	$e^{-\hat{T}_1}\hat{H}e^{\hat{T}_1}$	$\hat{T}_1$-transformed Hamiltonian
$\tilde{h}_{pq}$		$\hat{T}_1$-transformed one-integral
$\tilde{g}_{pqrs}$		$\hat{T}_1$-transformed two-integral
$\|\mathbf{c})$		Linear expansion of excited states
$\mathbf{H}$	$H_{\mu\nu} = (\mu\|\hat{H}\|\nu)$	Hamiltonian matrix
$\|\mu)$		General biorthonormal projection manifold
$\mathbf{c}$, $\overline{\mathbf{c}}$	c_μ, $\overline{c}_\mu$	Column vectors containing expansion coefficients
E_0		Ground state energy
$\boldsymbol{\eta}$	$(\text{R}\|\hat{H}\|\mu)$	Column vector
$\mathbf{A}$		Jacobian matrix
$A_{\mu\nu}$	Equation (19)	Elements of Jacobian matrix
$\Delta\mathbf{H}$	$\mathbf{H} - E_0\mathbf{1}$	Level-shifted Hamiltonian matrix
ΔE	$E - E_0$	Level-shifted energy
K		An excited state
$\mathbf{t}_K$, $\overline{\mathbf{t}}_K$		Column vectors containing expansion coefficients for excited states

Symbol	Definition	Description
$\mathbf{A}^{\mathrm{CCSD}}$	Matrix (22)	Jacobian matrix for CCSD
$\mathbf{A}^{\mathrm{CCSDT}}$	Matrix (23)	Jacobian matrix for CCSDT
$\mathbf{A}^{\mathrm{XPS}}$	Matrix (26)	Jacobian matrix for proposed model
$\hat{\tau}_{\nu_3}^{\mathrm{XPS}}$	$\hat{\tau}_{\nu_3}^{(1)} + \hat{\tau}_{\nu_3}^{(2)}$	Restricted triple excitation operator
$\left\langle \mu_3^{\mathrm{XPS}} \right\vert$		Restricted triple projection manifold
t^{XPS}		Excitation amplitudes for core excitation to super-diffuse orbital
$\hat{T}^{\mathrm{XPS}}$		Restricted triple contribution to $\hat{T}$
A, I		Fixed orbitals, core and super-diffuse orbital
P_{ij}^{ab}, P_{ijk}^{abc}	Equation (27), (28)	Double and triple permutation operators
A_{ij}^{ab}, A_{ijk}^{abc}		General integrals
Δ_{aibj}	$1 + \delta_{ai,bj}$	Constant
$\left\langle \overline{\substack{ab \\ ij}} \right\vert$		Biorthogonal states
$\left\langle \widetilde{\substack{ab \\ ij}} \right\vert$		Biorthonormal states
N_{ijk}^{abc}		Normalization constant for triple projection manifold
$\mathbf{c}_i$	$i = 1, 2, 3$	Column vectors for linear transformation coefficients
σ	Equation (29)	Linear transformation (LT)
$\sigma_{3,ai}$	$\rho_{3,ai}^{(1)} + \rho_{3,ai}^{(2)}$	LT of triple excitation, single projection manifold
$\sigma_{3,aibj}$	$\rho_{3,aibj}^{(1)} + \rho_{3,aibj}^{(2)}$	LT of triple excitation, double projection manifold
$\sigma_{3,aibjck}$	$\rho_{3,aibjck}^{(1)} + \rho_{3,aibjck}^{(2)}$	LT of triple excitation, triple projection manifold
$C_{bj,ck}^{AI}$		LT constants belonging to $\hat{\tau}_{\nu_3}^{(1)}$
$B_{b,j,dl}^{AI}$		LT constants belonging to $\hat{\tau}_{\nu_3}^{(2)}$
L_{bdlA}	$2g_{bdlA} - g_{bAld}$	Contraction of two-integrals
n_{occ}		Number of occupied orbitals
n_{vir}		Number of virtual orbitals

Symbol	Definition	Description
$\hat{A}$, $\hat{B}$, $\hat{C}$		General operators
F_{mn}	$h_{mn} + \sum_i (2g_{mnii} - g_{miin})$	Element of inactive Fock matrix
P_{ijkl}^{abcd}		Quadruple permutation operator
$s_{\hat{A}}^{-}$		Down rank of operator $\hat{A}$
$s_{\hat{A}}^{+}$		Up rank of operator $\hat{A}$
n_v^c		Number of virtual creation operators
n_o^a		Number of occupied annihilation operators
n_o^c		Number of occupied creation operators
n_v^a		Number of virtual annihilation operators
$m_{\hat{A}}$		Particle rank of $\hat{A}$
$s_{\hat{A}}$		Excitation rank of $\hat{A}$
$\hat{\Omega}$		Operator containing nested commutators
C_{bj}		LT constants belonging to $\hat{\tau}_{\nu_1}$
$C_{bj,ck}$		LT constants belonging to $\hat{\tau}_{\nu_2}$
$\tilde{C}_{bj,ck}$	$\Delta_{aibj} C_{ai,bj}$	Constant
$\tilde{C}_{bj,ck}^{AI}$	$\Delta_{aibj} C_{ai,bj}^{AI}$	Constant
c_{ij}	$i, j = 1, 2, 3, \ldots$	Elements of matrix $C_{bj,ck}$

Appendix A. Discrepancies between core-ionization energies for the CC(2,3) and the XPS-CCSD model

Table A.1 displays deviations in core-ionization energies for the modified CCSDT model, CC(2,3), and the XPS-CCSD model for molecules H_2O, CO and NH_3 in basis sets aug-cc-pCVTZ and aug-cc-pCVQZ. The modified CCSDT calculation was performed by setting all ground state triple excitation amplitudes equal to zero and neglecting all excitations not involving at least one core excitation to a super-diffuse orbital. The CC(2,3) calculation was performed by Dr. D. A. Matthews at University of Texas, and the core-ionisation energies of both CC(2,3) and XPS-CCSD are given in Table 3.

Table A.1. Discrepancies between the CC(2,3) ionization energies and XPS-CCSD ionization energies for H_2O, CO and NH_3 for basis sets aug-cc-pCVTZ and aug-cc-pCVQZ. Energies are given in eV.

Basis set	Molecule	Difference CC(2,3) and XPS-CCSD
	H_2O	
aug-cc-pCVTZ		0.0003116
aug-cc-pCVQZ		0.0237476
	CO (C)	
aug-cc-pCVTZ		0.0001711
aug-cc-pCVQZ		0.0094327
	CO (O)	
aug-cc-pCVTZ		0.0003121
aug-cc-pCVQZ		0.0142748
	NH_3	
aug-cc-pCVTZ		0.0002334
aug-cc-pCVQZ		0.0280239

Appendix B. Commutator relations and the BCH-expansion

When $\hat{A}$, $\hat{B}$ and $\hat{C}$ denote operators, the following commutation relations are valid

$$[\hat{A}, \hat{B}\hat{C}] = [\hat{A}, \hat{B}]\hat{C} + \hat{B}[\hat{A}, \hat{C}],$$

$$[\hat{A}, \hat{B}] = -[\hat{B}, \hat{A}].$$

In addition, when E_{pq} denotes a singlet excitation operator, $\tilde{H}$ the electronic $\hat{T}_1$-transformed Hamiltonian and δ_{pq} the Kronecker δ-function, the nested commutator $[E_{ck}[\tilde{H}, E_{dl}], E_{bj}]$ may be written as

$$\begin{aligned}
[E_{ck}[\tilde{H}, E_{dl}], E_{bj}] &= -([E_{bj}, E_{ck}][\tilde{H}, E_{dl}] + E_{ck}[E_{bj}, [\tilde{H}, E_{dl}]]) \\
&= E_{ck}[[\tilde{H}, E_{dl}], E_{bj}] + [E_{ck}, E_{bj}][\tilde{H}, E_{dl}] \\
&= E_{ck}[[\tilde{H}, E_{dl}], E_{bj}].
\end{aligned}$$

The last equality in the above expression is due to that $[E_{ck}, E_{bj}] = E_{cj}\delta_{bk} - E_{bk}\delta_{cj} = 0$ since $\delta_{bk} = 0$ and $\delta_{cj} = 0$. An occupied orbital and a virtual orbital can not be the same orbital.

According to Helgaker *et al.* the BCH-expansion, where BCH is an acronym for Baker-Campbell-Hausdorff[82], is defined as the following

$$e^{-\hat{A}}\hat{B}e^{\hat{A}} = \hat{B} + [\hat{B}, \hat{A}] + \frac{1}{2}[[\hat{B}, \hat{A}], \hat{A}] + \frac{1}{3!}[[[\hat{B}, \hat{A}], \hat{A}], \hat{A}] + \dots \ . \tag{B.1}$$

Appendix C. Non-zero commutators of the Hamiltonian and the single excitation operators applied to the Hartree-Fock state

The non-zero commutators of the Hamiltonian and the single excitation operators applied to the Hartree-Fock state is given below. These relations are given in Box 13.2 of *Molecular Electronic-Structure Theory*[26].

$$\tilde{H}\left|\mathrm{HF}\right\rangle = \sum_i (h_{ii} + F_{ii})\left|\mathrm{HF}\right\rangle + \sum_{ai} F_{ai}E_{ai}\left|\mathrm{HF}\right\rangle + \frac{1}{2}\sum_{aibj} g_{aibj}E_{ai}E_{bj}\left|\mathrm{HF}\right\rangle$$

$$[\tilde{H}, E_{ai}]\left|\mathrm{HF}\right\rangle = 2F_{ia}\left|\mathrm{HF}\right\rangle + \left(\sum_b F_{ba}E_{bi} - \sum_j F_{ij}E_{aj} + \sum_{bj} L_{bjia}E_{bj}\right)\left|\mathrm{HF}\right\rangle + \left(\sum_{bjc} g_{bjca}E_{bj}E_{ci} - \sum_{bjk} g_{bjik}E_{bj}E_{ak}\right)\left|\mathrm{HF}\right\rangle$$

$$\begin{aligned}[[\tilde{H}, E_{ai}], E_{bj}]\left|\mathrm{HF}\right\rangle = {} & 2L_{iajb}\left|\mathrm{HF}\right\rangle \\ & - P_{ij}^{ab}\left(F_{ib}E_{aj} + \sum_k L_{ikjb}E_{ak} - \sum_c L_{cajb}E_{ci}\right)\left|\mathrm{HF}\right\rangle \\ & - P_{ij}^{ab}\left(\sum_{ck} g_{ibck}E_{aj}E_{ck} + \sum_{ck} g_{ikcb}E_{ak}E_{cj}\right)\left|\mathrm{HF}\right\rangle \\ & + \left(\sum_{kl} g_{ikjl}E_{ak}E_{bl} + \sum_{cd} g_{cadb}E_{ci}E_{dj}\right)\left|\mathrm{HF}\right\rangle\end{aligned}$$

$$\begin{aligned}[[[\tilde{H}, E_{ai}], E_{bj}], E_{ck}]\left|\mathrm{HF}\right\rangle = {} & -P_{ijk}^{abc}L_{jbic}E_{ak}\left|\mathrm{HF}\right\rangle \\ & P_{ijk}^{abc}\left(\sum_l g_{iljc}E_{al}E_{bk} - \sum_d g_{ibdc}E_{aj}E_{dk}\right)\left|\mathrm{HF}\right\rangle\end{aligned}$$

$$\begin{aligned}[[[[\tilde{H}, E_{ai}], E_{bj}], E_{ck}], E_{dl}]\left|\mathrm{HF}\right\rangle &= P_{ijk}^{abc}(g_{kbid}E_{cl}E_{al} + g_{lbic}E_{dj}E_{ak}\left|\mathrm{HF}\right\rangle \\ &= \frac{1}{2}P_{ijkl}^{abcd}g_{idjc}E_{al}E_{bk}\left|\mathrm{HF}\right\rangle\end{aligned}$$

$\tilde{H}$ denotes the $\hat{T}_1$-transformed electronic Hamiltonian, $|\mathrm{HF}\rangle$ the Hartree-Fock state, which is used as a reference state, h_{pq} the one-electron integral, $F_{mn} = h_{mn} + \sum_i (2g_{mnii} - g_{miin})$ the inactive Fock matrix, E_{pq} the singlet excitation operator, g_{pqrs} the two-electron integral, where $L_{pqrs} = 2g_{pqrs} - g_{psrq}$. While P_{ij}^{ab}, P_{ijk}^{abc} and P_{ijkl}^{abcd} denote permutation operators.

Appendix D. Rank

In order to determine whether a nested commutator is equal to zero or not, the rank of the operator can be used. The down rank of an operator $\hat{A}$, $s^-_{\hat{A}}$, and the up rank of the same operator, $s^+_{\hat{A}}$, are defined as the following

$$s^+_{\hat{A}} = \frac{1}{2}(n^c_v + n^a_o),$$
$$s^-_{\hat{A}} = \frac{1}{2}(n^c_o + n^a_v),$$

where n^c_v denotes the number of virtual creation operators that $\hat{A}$ consists of and n^a_o the number of occupied annihilation operators that $\hat{A}$ consists of. Likewise, n^c_o and n^a_v denote the number of occupied creation operators and the number of virtual annihilation operators in $\hat{A}$. The particle rank, $m_{\hat{A}}$, and excitation rank, $s_{\hat{A}}$, of the operator $\hat{A}$ are defined as

$$m_{\hat{A}} = s^+_{\hat{A}} + s^-_{\hat{A}},$$
$$s_{\hat{A}} = s^+_{\hat{A}} - s^-_{\hat{A}}.$$

It follows that the numbers of nested commutators, k, have to be less than 2 two times the down rank of the operator,

$$2s^-_{\hat{A}} \geq k, \tag{D.1}$$

for the expression not to be equal to zero. This means that the nested commutator on the form

$$\hat{\Omega} = [[..[[\hat{A}, \hat{T}_{n_1}], \hat{T}_{n_2}], ...], \hat{T}_{n_k}],$$

vanishes if the number of nested commutators is greater than two times the down rank of the operator[26]. $\hat{T}_{n_i}$ denotes terms of the cluster operator, where $n_i = 1, 2, \ldots, N$ and $i = 1, 2, \ldots, k$. N denoting the number of electrons in the system.

Appendix E. Procedure used to derive the elements of the Jacobian matrix for the XPS-CCSD case

The following procedure is made use of when determining expressions of the linear transformed XPS-CCSD Jacobian matrix, see Equation (29) and Matrix (26). The procedure is given below.

(1) The linear transformation of the XPS-CCSD Jacobian matrix is given in Equation (29) and was further partitioned in Equations (30) and (31). Note that for each of the excitation operators, the projection manifold is single, double and the restricted triple manifold. In addition, the Hamiltonian is the similarity transformed Hamiltonian, $\hat{H}^{\mathrm{T}} = e^{-\hat{T}}\hat{H}e^{\hat{T}}$.

(2) The Hamiltonian is $\hat{T}_1$-transformed, see Equation (13), and expanded in accordance with the BCH-expansion, see Expression (B.1) in Appendix B.

(3) The expansion is inserted into the expression of the linear transformed elements, and the expression is further developed by noting that the nested commutators at some point in the expansion vanish to due the rank of the Hamiltonian, see Appendix D.

(4) The commutators that survive are rewritten to the form of the commutators in Appendix C in order to make use of the relations given in this appendix. This step involves making use of the relations given in Appendix B.

(5) When the commutators are on the warranted form the relations given in Appendix C are made use of. Note that the bra-projection manifold is biorthonormal, such that the biorthonormal states produce a normalization constant and a permutation operator, for instance it produces $N_{ijk}^{abc}P_{ijk}^{abc}$ for the triple projection manifold, as mentioned in Chapter 4.

(6) The terms of the expression are now contracted by using the properties of the Kronecker δ-functions that appear in the expressions. Thereby the expression is further contracted by switching dummy indices and collecting terms that sums over the same indices.

(7) The final expression for a linear transformed Jacobian matrix element is obtained by adding all the terms that emerge from all the surviving commutators.

Appendix F. Elements of the Jacobian matrix for the XPS-CCSD model

The derived expressions of the XPS-CCSD Jacobian matrix, see Equation (29) and Matrix (26) in Chapter 4, are given below. Note that a linear transformation is conducted by multiplying the Jacobian matrix, $\mathbf{A}^{\mathrm{XPS}}$, with coefficients matrix $\mathbf{c}$. This transformation is denoted as σ and has the form

$$\sigma = \mathbf{A}^{\mathrm{XPS}}\mathbf{c} = \mathbf{A}^{\mathrm{XPS}}\mathbf{c_1} + \mathbf{A}^{\mathrm{XPS}}\mathbf{c_2} + \mathbf{A}^{\mathrm{XPS}}\mathbf{c_3}^{(1)} + \mathbf{A}^{\mathrm{XPS}}\mathbf{c_3}^{(2)} = \sigma_1 + \sigma_2 + \sigma_3,$$

where

$$\sigma_\gamma = \sigma_{\gamma,ai} + \sigma_{\gamma,aibj} + \sigma_{\gamma,aibjck}, \qquad \text{for} \quad \gamma = 1, 2$$

$$\begin{aligned}\sigma_3 &= \sigma_{3,ai} + \sigma_{3,aibj} + \sigma_{3,aibjck} \\ &= \rho^{(1)}_{3,ai} + \rho^{(2)}_{3,ai} + \rho^{(1)}_{3,aibj} + \rho^{(2)}_{3,aibj} + \rho^{(1)}_{3,aibjck} + \rho^{(2)}_{3,aibjck}.\end{aligned}$$

There are two possible projection operators and projection manifolds for the triple excitation process, thereby $\sigma_{3,ai}$, $\sigma_{3,aibj}$ and $\sigma_{3,aibjck}$ are parted into two terms denoted by $\rho^{(1)}_{3,\ldots}$ and $\rho^{(2)}_{3,\ldots}$. The starting point for $\sigma_{1,ai}$ is $\sum_{bj} \left\langle {}^{\widetilde{a}}_{i} \right| [\hat{H}^T, E_{bj}] \left| \mathrm{HF} \right\rangle C_{bj}$ in accordance with the linear transformation, the definition of the Jacobian elements, see Equation (19), and the projection manifold. Making use of the BCH-expansion given in Appendix B and commutator relations given in Appendix C, the first term may be written as

$$\begin{aligned}\sigma_{1,ai} = &\sum_b F_{ab}C_{bi} - \sum_j F_{ji}C_{aj} + \sum_{bj} L_{aijb}C_{bj} \\ &+ \sum_{bjck} \Big(u^{ac}_{ik}C_{bj} - t^{cb}_{ki}C_{aj} - t^{ac}_{jk}C_{bi} \Big) L_{kcjb}.\end{aligned}$$

In the same manner, the second term of σ_1 has staring point $\sum_{ck} \langle \widetilde{{}^{ab}_{ij}} | [\hat{H}^T, E_{ck}] | \mathrm{HF} \rangle C_{ck}$ and may be written as

$$\begin{aligned}\sigma_{1,aibj} = \frac{1}{\Delta_{aibj}} P^{ab}_{ij} \Bigg[& \sum_c g_{aibc} C_{cj} - \sum_k g_{aikj} C_{bk} - \sum_{ck} F_{kc} (t^{ac}_{ij} C_{bk} + t^{ab}_{ik} C_{cj}) \\ & + \sum_{ckl} \Big(g_{kilc} (t^{ab}_{kl} C_{cj} + t^{bc}_{lj} C_{ak} + t^{ac}_{kj} C_{bl}) - L_{kjlc} (t^{ab}_{ik} C_{cl} + t^{ac}_{il} C_{bk}) \Big) \\ & - \sum_{ckd} \Big(g_{kdbc} (t^{ad}_{ki} C_{cj} + t^{dc}_{ij} C_{ak} + t^{ac}_{kj} C_{di}) \\ & - L_{kdbc} (t^{ac}_{ij} C_{dk} + t^{ad}_{ik} C_{cj}) \Big) \Bigg].\end{aligned}$$

The last term of σ_1 is single excitation within three occupied and three unoccupied orbitals and is expressed as $\sum_{dl} \langle \widetilde{{}^{abc}_{ijk}} | [\hat{H}^T, E_{dl}] | \mathrm{HF} \rangle C_{dl}$. This term takes the form

$$\begin{aligned}\sigma_{1,aibjck} = N^{abc}_{ijk} P^{abc}_{ijk} \Bigg[& - \sum_{dn} \Big(g_{ndck} (t^{ab}_{in} C_{dj} + t^{ad}_{ij} C_{bn}) + g_{njcd} (t^{ab}_{in} C_{dk} + t^{ad}_{ik} C_{bn}) \Big) \\ & + \sum_{ln} t^{ab}_{in} g_{njlk} C_{cl} + \sum_{df} t^{af}_{ij} g_{bfcd} C_{dk} \\ & + \sum_{dlfn} \Big(g_{lfnd} (t^{cf}_{nj} t^{ba}_{li} C_{dk} + t^{cb}_{nl} t^{fa}_{ji} C_{dk} + t^{cf}_{nj} t^{da}_{ki} C_{bl} + t^{bf}_{lj} t^{ca}_{ni} C_{dk} \\ & + t^{cf}_{lk} t^{da}_{ji} C_{bn} + t^{df}_{jk} t^{ca}_{li} C_{bn}) - L_{nfld} (t^{fb}_{nj} t^{ca}_{li} C_{dk} + t^{fb}_{nj} t^{da}_{ki} C_{cl} \\ & + t^{cb}_{nj} t^{fa}_{ki} C_{dl}) \Big) \Bigg].\end{aligned}$$

The first term of σ_2 has starting point $\sum_{bj \geq ck} \langle \widetilde{{}^{a}_{i}} | [\hat{H}^T, E_{bj} E_{ck}] | \mathrm{HF} \rangle C_{bj,ck}$ and have the form

$$\sigma_{2,ai} = \sum_{bj} F_{jb} (2\tilde{C}_{ai,bj} - \tilde{C}_{aj,bi}) - \sum_{bjk} L_{kijb} \tilde{C}_{bj,ak} + \sum_{bjc} L_{acjb} \tilde{C}_{bj,ci},$$

where $\tilde{C}_{ai,bj} = \Delta_{aibj} C_{ai,bj}$.

In the same manner, the second term of σ_2 may be written as $\sum_{ck\geq dl} \langle \widetilde{{}^{ab}_{ij}} | [\hat{H}^T, E_{ck}E_{dl}] | \mathrm{HF} \rangle C_{ck,dl}$ and can be expressed as

$$\begin{aligned}
\sigma_{2,aibj} = \frac{1}{\Delta_{aibj}} P^{ab}_{ij} \Bigg[& \sum_d F_{bd} \tilde{C}_{ai,dj} - \sum_l F_{lj} \tilde{C}_{ai,bl} \\
& + \sum_{dl} (L_{bjld} \tilde{C}_{ai,dl} - g_{ldbj} \tilde{C}_{al,di} - g_{libd} \tilde{C}_{al,dj}) \\
& + \frac{1}{2} \Bigg(\sum_{kl} g_{kilj} \tilde{C}_{ak,bl} + \sum_{cd} g_{acbd} \tilde{C}_{ci,dj} \Bigg) \\
& + \sum_{ckdl} \Bigg(\frac{1}{2} g_{kcld} (t^{bc}_{li} \tilde{C}_{ak,dj} + t^{ba}_{lk} \tilde{C}_{ci,dj} + t^{ca}_{ik} \tilde{C}_{bl,dj} \\
& + t^{bd}_{ki} \tilde{C}_{cj,al} + t^{bd}_{lj} \tilde{C}_{ci,ak} + t^{cd}_{ij} \tilde{C}_{bl,ak}) \\
& - L_{kcld} (t^{ad}_{il} \tilde{C}_{cj,bk} + t^{ac}_{ij} \tilde{C}_{bk,dl} + t^{ab}_{ik} \tilde{C}_{cj,dl} + t^{bc}_{lk} \tilde{C}_{ai,dj} \\
& + t^{cd}_{jl} \tilde{C}_{ai,bk} + t^{bc}_{kj} \tilde{C}_{ai,dl} - 2 t^{bc}_{jk} \tilde{C}_{ai,dl}) \Bigg) \Bigg].
\end{aligned}$$

The last term of σ_2 may be written as $\sum_{dl\geq em} \langle \widetilde{{}^{abc}_{ijk}} | [\hat{H}^T, E_{dl}E_{em}] | \mathrm{HF} \rangle C_{dl,em}$ and in the same manner as the previous terms, this term may be expressed as

$$\begin{aligned}
\sigma_{2,aibjck} = N^{abc}_{ijk} P^{abc}_{ijk} \Bigg[& \sum_d g_{bjcd} \tilde{C}_{dk,ai} - \sum_l g_{bjlk} \tilde{C}_{cl,ai} \\
& - \sum_{dl} F_{ld} (t^{cb}_{lj} \tilde{C}_{ai,dk} + t^{db}_{kj} \tilde{C}_{ai,cl}) \\
& + \sum_{dln} \Bigg(g_{njld} (t^{ba}_{ni} \tilde{C}_{cl,dk} + t^{da}_{ki} \tilde{C}_{bn,cl} + t^{bc}_{nl} \tilde{C}_{ai,dk} \\
& + t^{ca}_{li} \tilde{C}_{bn,dk} + t^{bd}_{nk} \tilde{C}_{ai,cl} + t^{dc}_{kl} \tilde{C}_{ai,bn}) \\
& - L_{nkld} (t^{cb}_{nj} \tilde{C}_{ai,dl} + t^{db}_{lj} \tilde{C}_{ai,cn}) \Bigg) \\
& - \sum_{dlf} \Bigg(g_{cfld} (t^{ba}_{li} \tilde{C}_{dj,fk} + t^{fa}_{ki} \tilde{C}_{bl,dj} + t^{da}_{ji} \tilde{C}_{bl,fk} \\
& + t^{bd}_{lj} \tilde{C}_{ai,fk} + t^{bf}_{lk} \tilde{C}_{ai,dj} + t^{fd}_{kj} \tilde{C}_{ai,bl}) \\
& - L_{cfld} (t^{fb}_{kj} \tilde{C}_{ai,dl} + t^{db}_{lj} \tilde{C}_{ai,fk}) \Bigg) \Bigg].
\end{aligned}$$

Remember that $\sigma_{3,ai}$ is divided into two terms in order to simplify the notation, $\sigma_{3,ai} = \rho^{(1)}_{3,ai} + \rho^{(2)}_{3,ai}$. The first term is expressed as $\sum_{bj \geq ck} \langle \widetilde{{}^{a}_{i}} | [\hat{H}^T, E_{AI} E_{bj} E_{ck}] | \mathrm{HF} \rangle C^{AI}_{bj,ck}$ and may be written as

$$\begin{aligned}\rho^{(1)}_{3,ai} = &- \sum_{bj} (L_{IAjb} \tilde{C}'^{AI}_{bi,aj} - 2L_{IAjb} \tilde{C}'^{AI}_{ai,bj}) - \sum_{jck} L_{kcjA} \tilde{C}'^{Ai}_{aj,ck} \\ &- \sum_{bjc} L_{jbIc} \tilde{C}'^{aI}_{ci,bj} + \sum_{bjck} L_{jbkc} \tilde{C}'^{ai}_{bj,ck},\end{aligned}$$

where $\tilde{C}'^{AI}_{bi,aj} = \Delta_{biaj} C^{AI}_{bi,aj}$. $\rho^{(2)}_{3,ai}$ is on the form $\sum_{bjck} \langle \widetilde{{}^{a}_{i}} | [\hat{H}^T, E_{Aj} E_{bI} E_{ck}] | \mathrm{HF} \rangle B^{AI}_{b,j,ck}$ and may be expressed as

$$\begin{aligned}\rho^{(2)}_{3,ai} = &- \sum_{bjck} L_{kcjb} B^{ai}_{b,j,ck} + \sum_{bjc} L_{Ibjc} (2B^{AI}_{b,i,cj} - B^{AI}_{b,j,ci}) \\ &+ \sum_{bjk} L_{jAkb} (2B^{Ai}_{a,j,bk} - B^{Ai}_{b,j,ak}) - \sum_{bk} (L_{IbkA} (B^{AI}_{b,i,ak} + B^{AI}_{a,k,bi} - 2B^{AI}_{b,k,ai}) \\ &+ L_{kbIA} B^{AI}_{a,i,bk}).\end{aligned}$$

The second term of σ_3 is also divided into two terms, $\sigma_{3,aibj} = \rho^{(1)}_{3,aibj} + \rho^{(2)}_{3,aibj}$, where the first term may be written as $\sum_{ck \geq dl} \langle \widetilde{{}^{ab}_{ij}} | [\hat{H}^T, E_{AI} E_{ck} E_{dl}] | \mathrm{HF} \rangle C^{AI}_{ck,dl}$ and may be rewritten as

$$\begin{aligned}\rho^{(1)}_{3,aibj} = \frac{1}{\Delta_{aibj}} P^{ab}_{ij} \Bigg[&\sum_{dl} F_{ld} (2\tilde{C}'^{ai}_{bj,dl} - \tilde{C}'^{ai}_{bl,dj}) - \sum_{kdl} L_{kjld} \tilde{C}'^{ai}_{dl,bk} + \sum_{cdl} L_{bcld} \tilde{C}'^{ai}_{dl,cj} \\ &- \sum_{cd} g_{Icbd} \tilde{C}'^{aI}_{ci,dj} - \sum_{dl} (L_{Iild} \tilde{C}'^{aI}_{bj,dl} - g_{Iild} \tilde{C}'^{aI}_{bl,dj} - g_{ljId} \tilde{C}'^{aI}_{bl,di}) \\ &- \sum_{d} F_{Id} \tilde{C}'^{aI}_{bj,di} + \sum_{kl} g_{kilA} \tilde{C}'^{Aj}_{ak,bl} \\ &- \sum_{dl} (g_{lAad} \tilde{C}'^{Aj}_{bl,di} + g_{ldbA} \tilde{C}'^{Aj}_{al,di} - L_{bAld} \tilde{C}'^{Aj}_{ai,dl}) \\ &- \sum_{l} F_{lA} \tilde{C}'^{Aj}_{ai,bl} + \sum_{d} L_{bdIA} \tilde{C}'^{AI}_{ai,dj} - \sum_{l} L_{ljIA} \tilde{C}'^{AI}_{ai,bl} + F_{IA} \tilde{C}'^{AI}_{ai,bj} \Bigg].\end{aligned}$$

$\rho^{(2)}_{3,aibj}$ is written as $\sum_{ckdl} \langle \widetilde{{}^{ab}_{ij}} | [\hat{H}^T, E_{Ak}E_{cI}E_{dl}] | \mathrm{HF} \rangle B^{AI}_{c,k,dl}$ and may be rewritten as

$$
\begin{aligned}
\rho^{(2)}_{3,aibj} = \frac{P^{ab}_{ij}}{\Delta_{aibj}} \Bigg[& - F_{IA} B^{AI}_{b,j,ai} - \sum_{d} (g_{IdbA} B^{AI}_{a,j,di} - L_{bAId} B^{AI}_{d,j,ai} + g_{IAbd} B^{AI}_{a,i,dj}) \\
& + \sum_{l} (g_{IilA} B^{AI}_{a,j,bl} + g_{ljIA} B^{AI}_{a,i,bl} - L_{IjlA} B^{AI}_{b,l,ai}) \\
& + \sum_{dl} F_{ld} ((2B^{aj}_{b,i,dl} - B^{aj}_{d,i,bl}) - B^{bi}_{a,l,dj}) \\
& - \sum_{ckd} (g_{kdbc} B^{aj}_{c,k,di} - L_{bckd} B^{aj}_{c,i,dk}) + \sum_{dkl} (g_{kild} B^{aj}_{d,k,bl} - L_{kild} B^{aj}_{b,k,dl}) \\
& - \sum_{dl} F_{ld} B^{bj}_{d,l,ai} - \sum_{ckd} g_{kcad} B^{bj}_{c,k,di} + \sum_{dkl} g_{likd} B^{bj}_{d,k,al} \\
& + \sum_{d} F_{Id} (2B^{bI}_{d,j,ai} - B^{bI}_{a,j,di}) + \sum_{dl} (g_{ljId} B^{bI}_{a,l,di} - L_{ljId} B^{bI}_{d,l,ai}) \\
& + \sum_{cd} L_{adIc} B^{bI}_{c,j,di} + \sum_{dl} (g_{Iild} B^{bI}_{a,l,dj} - L_{liId} B^{bI}_{d,j,al} - L_{Iild} B^{bI}_{a,j,dl}) \\
& + \sum_{l} F_{lA} (2B^{Aj}_{b,l,ai} - B^{Aj}_{b,i,al}) - \sum_{dl} (g_{lAbd} B^{Aj}_{d,i,al} + g_{ldaA} B^{Aj}_{d,i,bl} \\
& - L_{aAld} B^{Aj}_{b,i,dl} - L_{bdlA} B^{Aj}_{d,l,ai} - L_{adlA} B^{Aj}_{b,l,di}) - \sum_{kl} L_{likA} B^{Aj}_{b,k,al} \Bigg].
\end{aligned}
$$

The last term of σ_3, where triple excitations involving three occupied and three unoccupied orbitals occur, is parted in the following manner $\sigma_{3,aibjck} = \rho^{(1)}_{3,aibjck} + \rho^{(2)}_{3,aibjck}$. The first term is expressed as $\sum_{dl \geq em} \langle \widetilde{^{abc}_{ijk}} | [\hat{H}^T, E_{AI} E_{dl} E_{em}] | \mathrm{HF} \rangle \, C^{AI}_{dl,em}$ and may be rewritten as

$$
\begin{aligned}
\rho^{(1)}_{3,aibjck} = N^{abc}_{ijk} P^{abc}_{ijk} \Bigg[& \frac{1}{2} \Bigg(F_{cA} \tilde{C}^{Ak}_{ai,bj} - F_{Ik} \tilde{C}^{cI}_{ai,bj} + L_{ckIA} \tilde{C}^{AI}_{ai,bj} \Bigg) \\
& + \sum_{e} \Bigg(F_{ce} \tilde{C}^{ai}_{bj,ek} - g_{Ieck} \tilde{C}^{bI}_{ai,ej} - g_{Ijce} \tilde{C}^{bI}_{ai,ek} + g_{bAce} \tilde{C}^{Aj}_{ai,ek} \Bigg) \\
& - \sum_{m} \Bigg(F_{mk} \tilde{C}^{ai}_{bj,cm} + g_{mAck} \tilde{C}^{Aj}_{ai,bm} + g_{mjcA} \tilde{C}^{Ak}_{ai,bm} - g_{Ijmk} \tilde{C}^{bI}_{ai,cm} \Bigg) \\
& - \sum_{em} \Bigg(g_{meck} \tilde{C}^{ai}_{bm,ej} + g_{mjce} \tilde{C}^{ai}_{bm,ek} - L_{ckme} \tilde{C}^{ai}_{bj,em} \\
& + L_{IAme} (t^{bc}_{jm} \tilde{C}^{AI}_{ai,ek} + t^{be}_{jk} \tilde{C}^{AI}_{ai,cm} + \frac{1}{2} t^{ce}_{mk} \tilde{C}^{AI}_{ai,bj} - t^{ce}_{km} \tilde{C}^{AI}_{ai,bj}) \Bigg) \\
& + \frac{1}{2} \Bigg(\sum_{lm} g_{ljmk} \tilde{C}^{ai}_{bl,cm} + \sum_{de} g_{bdce} \tilde{C}^{ai}_{dj,ek} \Bigg) \\
& + \sum_{dle} \Bigg(g_{Idle} (t^{ac}_{il} \tilde{C}^{bI}_{dj,ek} + t^{ad}_{ij} \tilde{C}^{bI}_{cl,ek} + t^{ae}_{ij} \tilde{C}^{cI}_{dk,bl} + t^{cd}_{lj} \tilde{C}^{bI}_{ai,ek} \\
& + t^{be}_{lj} \tilde{C}^{cI}_{ai,dk} + t^{ed}_{jk} \tilde{C}^{cI}_{ai,bl}) - L_{ldIe} (t^{be}_{jk} \tilde{C}^{cI}_{ai,dl} + t^{bd}_{jl} \tilde{C}^{cI}_{ai,ek} + \frac{1}{2} t^{de}_{lk} \tilde{C}^{cI}_{ai,bj}) \Bigg) \\
& + \sum_{dlm} \Bigg(g_{mAld} (t^{ab}_{im} \tilde{C}^{Aj}_{cl,dk} + t^{ad}_{ik} \tilde{C}^{Aj}_{cl,bm} + t^{ac}_{il} \tilde{C}^{Aj}_{bm,dk} + t^{bc}_{ml} \tilde{C}^{Aj}_{ai,ek} \\
& + t^{cd}_{mj} \tilde{C}^{Ak}_{ai,bl} + t^{cd}_{lk} \tilde{C}^{Aj}_{ai,bm}) - L_{mdlA} (t^{bc}_{jl} \tilde{C}^{Ak}_{ai,dm} + t^{bd}_{jm} \tilde{C}^{Ak}_{ai,cl} + \frac{1}{2} t^{cd}_{lm} \tilde{C}^{Ak}_{ai,bj}) \Bigg) \\
& + \sum_{dlem} \Bigg(g_{ldme} (t^{cd}_{mj} \tilde{C}^{ai}_{bl,ek} + t^{db}_{jl} \tilde{C}^{ai}_{cm,ek} + \frac{1}{2} (t^{cb}_{ml} \tilde{C}^{ai}_{dj,ek} + t^{ed}_{jk} \tilde{C}^{ai}_{cl,bm}) \\
& - L_{ldme} (t^{cd}_{ml} \tilde{C}^{ai}_{bj,ek} + t^{ed}_{kl} \tilde{C}^{ai}_{bj,cm} + t^{bc}_{jl} \tilde{C}^{ai}_{dk,em} + t^{bd}_{jk} \tilde{C}^{ai}_{cl,em} \\
& + t^{bd}_{jl} \tilde{C}^{ai}_{cm,ek} + \tilde{C}^{ai}_{bj,em} (t^{cd}_{lk} - 2 t^{cd}_{kl})) \Bigg] .
\end{aligned}
$$

The last term, $\rho^{(2)}_{3,aibjck}$, is expressed as
$\sum_{dlem} \langle \widetilde{^{abc}_{ijk}} | [\hat{H}^T, E_{Al}E_{dI}E_{em}] | \mathrm{HF} \rangle B^{AI}_{d,l,em}$ and may be rewritten to an enormous term that stretches over two pages

$$
\begin{aligned}
\rho^{(2)}_{3,aibjck} = N^{abc}_{ijk} P^{abc}_{ijk} \Bigg[& F_{cA} B^{Ai}_{a,k,bj} - F_{Ik} B^{aI}_{c,i,bj} - g_{IAck} B^{AI}_{b,j,ai} - g_{IjcA} B^{AI}_{b,k,ai} \\
& + \sum_e \Bigg(F_{ce}(B^{aj}_{b,i,ek} + B^{ak}_{e,i,bj}) - g_{Ieck} B^{aI}_{b,i,ej} - g_{Ijce} B^{aI}_{b,i,ek} \\
& + g_{bAce}(B^{Ak}_{e,j,ai} - B^{Ai}_{a,j,ek}) + L_{ckIe} B^{aI}_{e,i,bj} \Bigg) \\
& - \sum_m \Bigg(F_{mk}(B^{aj}_{b,i,cm} + B^{ci}_{a,m,bj}) - g_{Ijmk} B^{aI}_{b,i,cm} + g_{mAck} B^{Ai}_{a,j,bm} \\
& + g_{mjcA} B^{Ai}_{a,k,bm} - g_{mjIk} B^{bI}_{c,m,ai} - L_{ckmA} B^{Ai}_{a,m,bj} \Bigg) \\
& - \sum_{em} \Bigg(g_{meck}(B^{bi}_{a,m,ej} + B^{aj}_{e,i,bm} + B^{bj}_{e,m,ai}) \\
& + g_{mjce}(B^{bi}_{a,m,ek} + B^{ak}_{e,i,bm} + B^{bk}_{e,m,ai}) - L_{ckme} B^{aj}_{b,i,em} \\
& - g_{IAme}(t^{ac}_{im} B^{AI}_{b,j,ek} + t^{ae}_{ij} B^{AI}_{c,k,bm} + t^{ce}_{mk} B^{AI}_{b,j,ai}) \\
& - g_{mAIe}(t^{ab}_{im} B^{AI}_{c,j,ek} + t^{ae}_{ik} B^{AI}_{c,j,bm} + t^{ce}_{mj} B^{AI}_{b,k,ai}) \\
& + L_{IemA}(t^{bc}_{jm} B^{AI}_{e,k,ai} + t^{be}_{jk} B^{AI}_{c,m,ai}) + L_{meIA} t^{be}_{jm} B^{AI}_{c,k,ai} \Bigg) \\
& + \sum_{de} g_{bdce} B^{aj}_{d,i,ek} + \sum_{lm} g_{ljmk} B^{bi}_{a,l,cm} \\
& + \sum_{dle} \Bigg(g_{Idle}(t^{cd}_{lj} B^{aI}_{b,i,ek} + t^{eb}_{jl} B^{aI}_{c,i,dk} + t^{ae}_{ij} B^{bI}_{c,l,dk} \\
& + t^{ad}_{ij} B^{cI}_{b,l,ek} + t^{ed}_{jk} B^{aI}_{c,i,bl} + t^{de}_{jk} B^{cI}_{b,l,ai}) \\
& - L_{Idle}(t^{bc}_{jl} B^{aI}_{d,i,ek} + t^{bd}_{jk} B^{aI}_{c,i,el} + t^{be}_{jk} B^{aI}_{d,i,cl} + t^{be}_{jl} B^{aI}_{c,i,dk} \\
& + t^{ed}_{lk} B^{aI}_{c,i,bj} + B^{aI}_{d,i,bj}(t^{ce}_{lk} - 2t^{ce}_{kl}) + t^{be}_{jk} B^{cI}_{d,l,ai}) \Bigg)
\end{aligned}
$$

$$
\begin{aligned}
&+ \sum_{dlm} \Bigg(g_{mAld}(t^{ac}_{il} B^{Ak}_{d,j,bm} + t^{ac}_{im} B^{Aj}_{d,k,bl} + t^{cd}_{lk} B^{Ai}_{a,j,bm} \\
&+ t^{cb}_{lm} B^{Ai}_{a,j,dk} + t^{cd}_{mj} B^{Ai}_{a,k,bl} + t^{cb}_{lm} B^{Ak}_{d,j,ai}) \\
&- L_{mAld}(B^{Ai}_{a,m,bj}(t^{cd}_{lk} - 2t^{cd}_{kl}) + t^{cd}_{ml} B^{Ai}_{a,k,bj} + t^{bc}_{jl} B^{Ai}_{a,m,dk} \\
&+ t^{bd}_{jk} B^{Ai}_{a,m,cl} + t^{bd}_{jl} B^{Ai}_{a,k,cm} + t^{bc}_{jm} B^{Ai}_{a,k,dl} + t^{bc}_{jl} B^{Ak}_{d,m,ai}) \Bigg) \\
&+ \sum_{dlem} \Bigg(g_{ldme}(t^{ed}_{jk} B^{ci}_{a,l,bm} + t^{db}_{jl} B^{ci}_{a,m,ek} + t^{ac}_{im} B^{bj}_{d,l,ek} + t^{ae}_{ij} B^{ck}_{d,l,bm} \\
&+ t^{ab}_{im} B^{cj}_{e,l,dk} + t^{ad}_{ik} B^{cj}_{e,l,bm} + t^{cb}_{ml} B^{aj}_{d,i,ek} + t^{ce}_{mk} B^{aj}_{d,i,bl} \\
&+ t^{ce}_{lj} B^{ak}_{d,i,bm} + t^{be}_{mj} B^{ck}_{d,l,ai} + t^{cd}_{mj}(B^{bk}_{e,l,ai} + B^{bi}_{a,l,ek})) \\
&- L_{ldme}(B^{aj}_{b,i,em}(t^{cd}_{lk} - 2t^{cd}_{kl}) + t^{cd}_{ki} B^{aj}_{b,l,em} + t^{ce}_{km}(B^{aj}_{d,i,bl} + B^{aj}_{b,l,di}) + t^{eb}_{ml} B^{aj}_{d,i,ck} \\
&+ t^{be}_{jm} B^{ai}_{d,l,ck} + t^{cb}_{kl} B^{aj}_{d,i,em} + t^{dc}_{lm} B^{aj}_{b,i,ek} + t^{ed}_{mi} B^{aj}_{b,l,ck} + t^{de}_{lk} B^{aj}_{b,i,cm}) \Bigg) \Bigg].
\end{aligned}
$$

Appendix G. The linear transformation constants

In the case of a linear transformation where the double excitation operator is involved, $\hat{\tau}_{\nu_2}$ is for instance equal to $E_{ck}E_{dl}$, the linear transformation constants are denoted as $C_{bj,ck}$. These constants can be unwrapped as a symmetric matrix as

$$C_{bj,ck} = \begin{pmatrix} c_{11} & c_{12} & c_{13} \\ c_{21} & c_{22} & c_{23} \\ c_{31} & c_{32} & c_{33} \end{pmatrix}. \tag{G.1}$$

Since this matrix is a symmetric matrix, it means that $c_{12} = c_{21}$, $c_{13} = c_{31}$ and $c_{23} = c_{32}$. Thus, $C_{bj,ck}$ is equal to $C_{ck,bj}$. Due to the symmetry property, the summation over $bj \geq ck$ denotes all the elements in either the upper or lower triangle of Matrix (G.1). In order to rewrite the summation, note that

$$\frac{1}{2}\sum_{bjck} C_{bj,ck} = \frac{1}{2}(c_{11} + c_{22} + c_{33}) + c_{21} + c_{23} + c_{31},$$

which almost gives the lower triangle of the matrix. When modifying this result in order to give all the elements of the lower triangle, note that

$$\frac{1+\delta_{bj,ck}}{2} = \begin{cases} \frac{1}{2} & \text{if } bj \neq ck \\ 1 & \text{if } bj = ck. \end{cases}$$

Thereby, the summation over $bj \geq ck$ may be rewritten as the following

$$\sum_{bj \geq ck} C_{bj,ck} = \sum_{bjck} \frac{1+\delta_{bj,ck}}{2} C_{bj,ck} = \sum_{bjck} \frac{\Delta_{bj,ck}}{2} C_{bj,ck}. \tag{G.2}$$

When considering the linear transformation constants belonging to the triple excitation operator $\tau^{(1)}_{\nu_3}$, see Equation (24), these constants may be unwrapped as a symmetric matrix as in accordance with the constants for the double excitation, since the summation is only over $bj \geq ck$ in this case as well. Thus the same rewriting as in Equation (G.2) may be used. Considering the triple excitation operator $\tau^{(2)}_{\nu_3}$, see Equation (25), the constants $B^{AI}_{c,k,dl}$ emerge. It is not possible to unwrap these constants as a symmetric matrix, thus $B^{AI}_{b,j,ck} \neq B^{AI}_{c,k,bj}$. This non-symmetry is also emphasised in the notation of $B^{AI}_{b,j,ck}$, note the two commas in the subscript.